Journal of Materials Chemistry C

ROYAL SOCIETY OF CHEMISTRY

REVIEW

View Article Online
View Journal | View Issue

Cite this: J. Mater. Chem. C, 2023, 11, 6777

Recent advances in ecofriendly 2D monoelemental bismuthene as an emerging material for energy, catalysis and biomedical applications

Shwetharani R.,*[a] Itika Kainthla,[b] Sumanth Dongre S.,[a] Laveena D'Souza[c] and R. Geetha Balakrishna*[a]

Since the discovery of graphene, two-dimensional (2D) materials have been established as a vibrant research topic in the fields of energy and catalysis. Among them, 2D mono-elemental bismuthene has attracted interest from researchers owing to its unique electrical, mechanical, optical and chemical properties. In addition, low toxicity and biocompatibility make it a promising material for various applications, such as energy, optoelectronics, catalysis and biomedical sciences. 2D bismuthene with a large bulk gap is a good candidate as a room-temperature topological insulator, and it also exhibits high cyclability in battery application and displays air stability. Furthermore, its high surface area and excellent electrochemical activity make it a potential electrocatalyst for energy conversion. Thus, considering all the fascinating aspects of bismuthene, our aim is to exclusively review the recent advances in 2D monoelemental bismuthene, its properties, synthesis techniques and applications in energy, catalysis and biomedical sciences. This study initially gives an overview of its properties, such as structural, topological, conducting, chemical, carrier mobility, ferroelectric and thermal. Subsequently, we discuss the facile synthesis of bismuthene through chemical vapour deposition, physical vapour deposition, chemical exfoliation, mechanical exfoliation and liquid-phase exfoliation. Further, we present its applications in electrochemical and photocatalytic processes, such as hydrogen evolution reaction, sensing and CO_2 reduction, then in optoelectronics, supercapacitors, and batteries, and finally in biomedical applications.

Received 16th February 2023,
Accepted 26th April 2023

DOI: 10.1039/d3tc00587a

rsc.li/materials-c

1. Introduction

Comprehensive research has been directed towards the development of sustainable and efficient catalysts for energy and environmental applications. Two-dimensional (2D) materials have attracted significant attention from the scientific community for over a decade to address many issues in energy, electronics and health care[1,2] owing to their unique properties, such as high charge carrier mobility, excellent flexibility and large mechanical robustness.[1,3,4] Studies on 2D materials have been significantly influenced by graphene, which has been extensively studied over the years.[5,6] 2D nanostructured materials consist of a nano-size planar crystal structure with monolayer or few-layer assemblies. Presently, research is focused on developing various types of graphene-like 2D materials,[7] such as transition metal dichalcogenides (TMDs), mixed metal carbides (MXenes), layered oxides and mono-elemental materials (Xenes).[8] Among them, Xenes, which include group IVA and group VA[9] elements, such as carbon, silicon, germanium, tin, phosphorene, arsenene, bismuthene, and antimonene with fascinating features, such as high carrier mobility, superior specific surface area, low carrier density and in-plane anisotropy, make them a topic of interest.[10] Arsenene, bismuthene and antimonene were synthesized earlier; however, their research applications have only been explored recently. Group VA elements, which are known as pnictogens, show toxicity with arsenene being extremely toxic. Notably, bismuthene display lower toxicity compared to other conventional graphene and phosphorus derivatives[11] and biocompatibility based on the clinical biosafety data of bismuth-based drugs and its high stability under ambient conditions. Furthermore, bismuthene is an environmentally friendly material, which can be used in biomedical applications, besides the energy and catalysis fields. Importantly, bismuthene can be

[a] Centre for Nano and Material Sciences, Jain (Deemed-to-be University), Jain Global Campus, Kanakapura, Bangalore, 562112, Karnataka, India. E-mail: r.shwetha@jainuniversity.ac.in, br.geetha@jainuniversity.ac.in
[b] School of Physics and Material Sciences, Shoolini University, Bajhol, Himachal Pradesh, 173229, India
[c] St. Aloysius College (Autonomous), Mangalore, India

extended to large-scale production and real-time applications owing to its low toxicity, high stability and environmental compatibility. Few-layered bismuthene (Bi) belongs to group VA, has a controlled energy band gap of almost 0 eV to 0.55 eV, manifests an excellent solar response, and its adjustable band gap has made it an appropriate candidate for various applications; thus it has been applied in biosensing, catalysis, gas sensing and biomedicine.[12–14] Bismuthene has a large atomic weight with strong spin orbit coupling and owns remarkable topological and metallic properties such as quick carrier mobility and durable light material interactions.[4,15,16] Studies have shown that the 2D form of bismuthene acts as a 2D topological insulator but this topic still under debate.[17] Bismuthene was discovered in 1997 on a Bi(111) surface and bismuth can form bismuthene with a planar or sp^2 honeycomb lattice.[13] Bismuthene tends to form a rhombohedral structure (β-phase), which is thermodynamically stable according to a DFT study. Bismuthene nanosheets possess a hexagonal buckled 2D structure with an improved lattice constant of a = 4.357 Å and bond distance between the Bi-Bi atoms in the Bi nanosheet of 3.04 Å.[26–29] Also, the bond angle and buckling height of the Bi nanosheet were found to be about 93.27° and 1.73 Å, respectively. The buckled structure of the Bi nanosheet stabilizes the layered nanostructure. An image of a bismuthene nanosheet is shown in Fig. 1.[13]

Bismuthene has attracted attention in a wide range of applications in various fields[18,19] (Fig. 2). Recently, the number of applications of bismuthene has expanded exponentially in terms of catalysis (water splitting, degradation, hydrogenation, and CO_2 reduction), biomedicine, polarized photodetection, neutral networks, electrochemistry and energy, electronics, photonics and logic transistors.[11,20] The enlarged surface and excellent electrochemical behavior of 2D bismuthene make it a good catalyst for CO_2 reduction and N_2 fixation. Furthermore, the air stability and low toxicity of bismuthene enable large scale/industrial applications. In this review, we present the properties, synthesis and applications of bismuthene in detail. Herein, initially, we present an overview on the properties of bismuthene including its structural, topological, conducting, chemical, carrier mobility, ferroelectric and thermal properties. Then, we discuss the facile synthesis of bismuthene through chemical vapour deposition, physical vapour deposition, chemical exfoliation, mechanical exfoliation and liquid phase exfoliation.[21,22] Further, we discuss its applications in electrochemical and photocatalytic processes such as hydrogen evolution reaction, sensing and CO_2 reduction, then in optoelectronics, supercapacitors, and batteries, and finally in biomedical applications. The future scope of nanoengineered 2D monoelemental bismuthene is also highlighted.

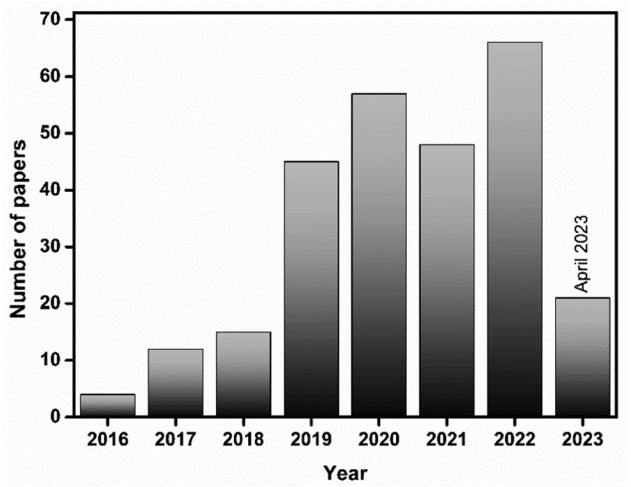

Fig. 2 Bar graph representing the number of publications *versus* year. Web of Science search data with the keyword "bismuthene".

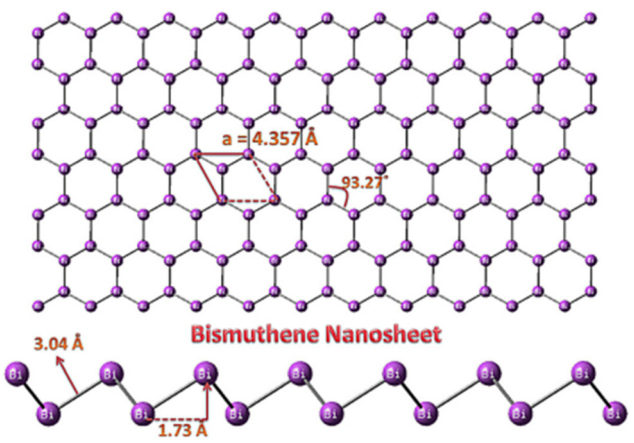

Fig. 1 Schematic of bismuthene nanosheet. Reprinted with permission from Elsevier.[13]

2. Properties

Bi, which is present in Group V, is the most metallic element in this group with a high mass fraction, making it unique. Density functional theory (DFT) calculation suggested that the rhombohedral structure of bismuthene is the only stable structure. The literature suggests that bismuthene may behave as an insulator with a 2D topological structure with spin–orbit monolayer and predicted bandgap of ≈0.3 eV and measured band gap of 0.67 eV, which disappear in multilayer bismuthene given that it becomes metallic; however this is still under debate. The conversion of semi-metal/metal through exfoliation into a semiconductor is associated with electron transfer and band gap transitions. Interestingly, a reduction in the thickness of Bi may lead to exceptional properties such as 2D topological insulation, which is not present in bulk Bi. Furthermore, the metallic and conductivity properties of bismuthene are dependent on its number of layers. In terms of chemical properties, the unpaired electron present in bismuthene is easily accessible compared to arsenene and antimonene, making it more suitable for sensing NH_3, NO and NO_2 through the formation of a strong metal-nitrogen covalent bond. The exfoliation of bismuthene consumes less energy than other Xenes due to its metallic nature and Bi has prominent spin–orbit coupling in its structure.

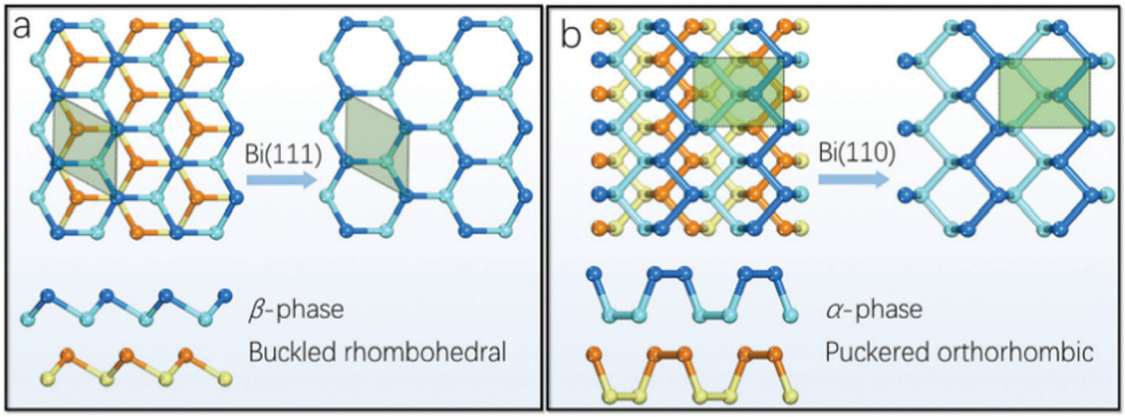

Fig. 3 (a) Top and side views of Bi(111), showing its buckled honeycomb structure. (b) Top and side views of Bi(110), showing puckered the black-phosphorus-style allotrope. Reprinted with permission from RSC.[23]

Bismuthene has a direct tunable band gap with high carrier mobility, similar to black phosphorus, and also exhibits high intrinsic stability in the ambient environment. Theoretical calculations suggest that the band gap of bismuthene is in the range of 0 to 0.55 eV, indicating its potential applications in the mid infrared (MIR) and infrared (IR) regions. Additionally, the buckled Bi(111) and puckered Bi(110) phases exhibit high air stability. The puckered structure (Fig. 3) of bismuthene exhibits ferroelectric and even antiferroelectric property with a Curie temperature above room temperature. The carrier transport properties of bismuthene determined through the deformation potential technique exhibited high values, reaching up to thousands of $cm^2 V^{-1} s^{-1}$. The effect of temperature on the armchair and zigzag structures of bismuthene suggests a significant reduction in these properties with an increase in temperature. The zigzag orientation exhibits excellent resistance, while the armchair exhibits shows better elasticity. Wang *et al.*[24] combined acid interaction and liquid separation and converted bulk bismuth into a multilayer semiconductor, which exhibited invisible optoelectronic properties (nonlinear response up to near IR). Bismuthene has been used in optical logic gates, fibre optics and laser material processing (Fig. 4). The thermal properties of bismuthene are influenced by temperature and presence of vacancies, where an increase in temperature and vacancies results in a decrease in thermal properties.[1] The interlayer spacing of monolayer bismuthene is 3.9 Å and exhibits reversible ion insertion and extraction.[25] Employing first principal calculations, Hong *et al.*[26] studied the ferroelectric polarization in monoelemental bismuthene nanoribbons and explained that their width size-limiting effect is due to edge stress effects. The decrease in width led to the spontaneous exchange of zigzag and armchair bismuthene to symmetric nonpolarized nanoribbons. To improve the various applications of 2D-based materials, altering their surface structure by anchoring or doping single-atom impurities has recently become a topic of research. Bismuthene may be doped with non-metal atoms, endowing it with a variety of electrical and magnetic properties, which can be used in spintronic devices. Recently, Nguyen *et al.* systematically examined the

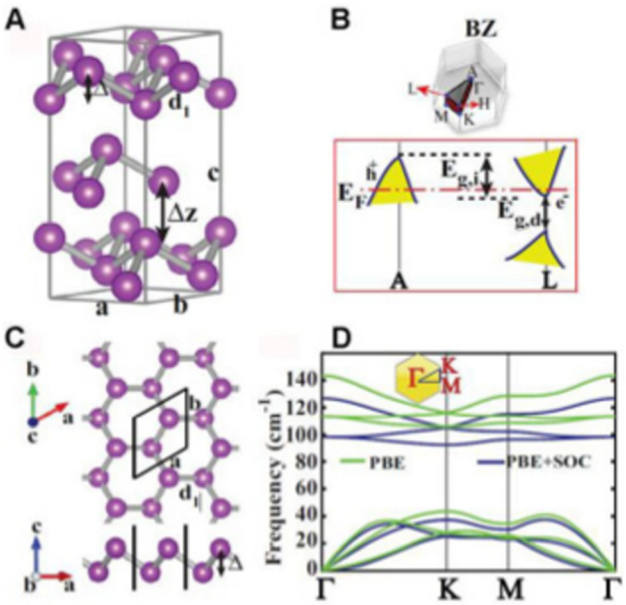

Fig. 4 (A) Hexagonal unit cell of bulk Bi structure, (B) related structure of Bi crystal, (C) single-layer of buckled honeycomb structure of Bi, b-Bi and (D) phonon dispersion curves calculated with and without spin–orbit coupling. Reprinted with permission from ACS.[12]

impact of group IVA atom (C, Si and Ge) doping on the structural, electrical, and magnetic characteristics of monolayer bismuthene using first-principles simulations. Due to the notable size difference between the dopant and host Bi atoms, their integration results in local structural deformation. This effect was observed to diminish as the number of atoms in the IVA group increases. Accordingly, the decrease in doping energy suggested that the doping process may require less energy and it has potential to marginally improve the existing electrical and magnetic properties of 2D bismuthene.[27] In a related study, Lopes and group compared transition metal-doped bulk and nanoribbon bismuthene using first-principles and a Hamiltonian model. To test the implications of the topological states on the magnetic interactions, they performed

simulations using the vanadium ion as a model of 3D transition metal-doped bismuthene. According to their findings, anti-ferromagnetism is dominant and is supported by the topological states, while spin-locked Dirac crossing states are preserved as a result of the general preservation of time-reversal symmetry. The spin diffusion length can be increased by the prolonged magnetic contacts, which are mostly mediated by massless electrons, which is encouraging for quick dissipation-free spintronic devices.[28] The properties of bismuthene nanosheets such as tunable bandgap, stability, and elasticity make it a unique amongst the two-dimensional materials. Thus, many researchers are using few-layer bismuthene nanosheets in various applications.

Overall, the crystal structure, lattice parameters, band structure, thickness, surface energy and strain of bismuthene contribute to its unique structural properties and make it a promising material for electronic and optoelectronic applications. However, the structural regulation of bismuthene materials is still in its infancy. One important aspect of the structural regulation of bismuthene materials is the control of their thickness and crystal orientation. This can be achieved through various preparation methods, which will be discussed in the following section, such as epitaxial growth on suitable substrates or chemical vapor deposition (CVD) technique. The resulting films can have different thicknesses and crystallographic orientations, which can affect their electronic and optical properties. Another important consideration in the structural regulation of bismuthene materials is the control of their defects and impurities, which can arise during the growth process or exposure to the environment and can significantly affect the electronic properties of the material. Therefore, it is important to develop methods for the controlled introduction of defects or the removal of impurities to optimize the properties of these materials. Further, the structural regulation of bismuthene can also involve the design of heterostructures and interfaces with other materials. By combining bismuthene with other materials, it is possible to create hybrid materials with unique properties that can be tailored based on the requirement.[29]

The structural regulation of 2D bismuthene can be achieved through various methods, as follows:

(i) Substrate engineering: bismuthene can be grown on different substrates, which can influence its structural properties. For example, the growth of bismuthene on a substrate with a mismatched lattice constant can induce strain, which can modify its electronic properties.

(ii) Doping: doping bismuthene with foreign atoms can alter its structural properties. For example, doping with carbon atoms can introduce defects in its lattice, which can modify its electronic and mechanical properties.

(iii) Chemical functionalization: bismuthene can be chemically functionalized with different molecules, which can modify its surface properties. For example, functionalizing bismuthene with halogens can passivate its surface, making it more stable and less prone to oxidation.

(iv) Mechanical deformation: bismuthene is highly susceptible to mechanical deformation, which can modify its structural and electronic properties. For example, applying strain can tune its bandgap and carrier mobility.

(v) Stacking: stacking multiple layers of bismuthene can create van der Waals heterostructures with unique structural properties.

Further, the method employed for the preparation of 2D bismuthene can have a significant influence on its structure, including its crystal structure, morphology, thickness, and defect density. The various methods for its preparation are discussed in the next section. The choice of method should be carefully considered based on the desired properties of bismuthene for a particular application.[8,30–32]

3. Preparation methods

The preparation of 2D bismuthene can follow the top-down or bottom-up approach. However, the former is more popular and involves exfoliating the bulk material, where the layers overlap with weak van der Waals interactions. This is carried out based on mechanical effects such as liquid-phase exfoliation, mechanical cleavage and etching. Among them, liquid-phase exfoliation is one of the most promising and popular techniques because of its potential to produce high yields of multilayer 2D-bismuthene. Alternatively, bottom-up methods convert ions, particles, or atoms directly into 2D-materials and involve methods such as thermal, vapor and plasma-assisted deposition and chemical synthesis. The vapour deposition methods for the growth of bismuthene are currently limited to pnictogens, and thus efforts are required to develop suitable procedures to enhance its efficacy. The choice of the optimal method to synthesize 2D bismuthene for energy applications depends on several factors such as the desired properties of the material, scalability, and cost-effectiveness of the synthesis method. Hence, some of the commonly used methods for the synthesis of 2D bismuthene with potential energy applications are briefly discussed in this section. The different methods reported for the experimental synthesis of bismuthene include various exfoliation, deposition, hot-pressing and wet-chemical methods.[17,33–38]

3.1. Mechanical and liquid-phase exfoliation

Mechanical exfoliation to fabricate 2D materials is well known due to its simple principle, wherein the van der Waals forces between the layers are broken by the adhesive force of a tape. This method follows a simple approach and the properties of the layered material are retained to a great extent. However, the underlying assumption of the mechanical exfoliation method is that the target layered semiconductor has good quality and weak van der Waals force, which has made the preparation of bismuthene challenging thus far. Furthermore, because the size, morphology, and other parameters of the samples obtained by mechanical exfoliation are not controllable, this approach is limited to research at the laboratory level.[34,39]

Liquid-phase exfoliation has evolved as the most significant top-down technique to prepare 2D bismuthene, given that it

overcomes the challenges of low yield and has better control of the growth than the mechanical exfoliation method. This approach has the merits of being cost-effective, highly efficient and operationally simple.[16,33] However, its drawbacks include low sample quality and difficulties in scaling up to industrial levels. The typical synthesis method involves the use of ultrasonic technology, such as ion intercalation, ion replacement, bath sonication, and tip sonication. The exfoliation of bulk bismuth into 2D-nanosheets involves initially placing the bulk materials in certain organic solvents under ultrasonic treatment, followed by centrifugation of the obtained dispersion several times to get a supernatant containing bismuthene. Given that this method includes molecular sizes smaller than 0.5 nm, H_2SO_4 is added to bismuthene with optimal geometrical factors and chemical affinities, leading to its exfoliation into ultrathin sheets. Reports revealed that the exfoliation effect is associated with the surface energy of the solvent, and thus it becomes important to choose a suitable organic solvent to achieve a stable dispersion of the obtained 2D materials in organic solution for an overall efficient exfoliation.[3,15,33,40] Chen *et al.* modified this simple method by using a pre-grinding liquid sonication exfoliation technique, and interestingly achieved better results. In their typical synthesis, prior to sonication, the Bi powder was placed in an agate mortar, the required amount of solvent added, and the sample ground for one hour. This pre-grinding produced shearing force along the layer surface, which promoted the generation of large and thin bismuth plates with a smooth surface. Further, a suspension was made by dispersing the mixture in the solvent and a surfactant (oleic acid) was added with subsequent sonication and centrifugation.[41] A similar strategy involving a two-step aqueous shear force exfoliation method was followed by Lazanas *et al.*, where the authors performed the shear dispersion and exfoliation of the bulk crystals in an aqueous sodium surfactant using a kitchen blender.[42] Other researchers have also reported this strategy to prepare 2D bismuthene for various applications.[43–45] Together with 2D-bismuthene nanosheets, bismuthene quantum dots are attracting interest from researchers due to their rich and fascinating properties owing to the quantum confinement effect. The liquid-phase exfoliation route has also been employed to synthesis BiQDs with a size of about 4 nm.[46–48] The exfoliation synthesis method can yield bismuthene with good properties but with little control of the size and number of layers, making it difficult to reproduce on a large scale. Thus, exfoliation may not be a suitable method to synthesize highly controlled bismuthene samples.

3.2. Hot-pressing method

The hot-pressing technique involves the simultaneous application of heat and pressure. This technique is versatile and has been also employed for the synthesis of bismuthene, as reported by Hussein *et al.* for the first time. According to researchers, it is a novel, facile, and cost-effective mechanical route employing large thermo-compression to prepare ultrathin bismuthene. In general, bismuth nanoparticles were compacted using an appropriate press, and simultaneously heated at a particular temperature.[49,50] However, it is difficult to determine the effectiveness of this synthesis technique, and thus more studies are required to explore its efficiency for the synthesis of bismuthene.

3.3. Molecular beam epitaxy method

Molecular beam epitaxy is a robust bottom-up approach, which has been widely applied to grow 2D materials. It is a simple method to achieve the high-quality, uniform and controlled growth of 2D Bi(110) and Bi(111) on a substrate. This method works under ultrahigh vacuum and relatively low temperatures compared to vapour-phase deposition.[50] Given that the topological quantum properties in 2D materials are greatly influenced by the film-substrate interactions and growth temperatures, it is important to symmetrically match the film and substrate during the epitaxial growth process. In this case, matching the index of monoelemental 2D bismuthene with the lattice substrate results in strong interfacial interactions, and consequently breaks the intrinsic topological properties by strong orbital hybridization with the substrate.[50] It has been established that metals on semiconductors and oxides prefer 3D growth modes rather than 2D films, which are known to be atomically smoother. However, deposition at low temperatures or surfactant-mediated growth can overcome this problem by modifying the kinetics of the film.[51] To control and monitor these parameters, *in situ* characterization methods, such as angle-resolved photoemission spectroscopy (ARPES), surface X-ray diffraction (SXRD), low-energy electron diffraction (LEED), and atomic force microscopy (AFM) measurements, are usually built-in in the vacuum chamber for time-on-stream analysis of the growth of 2D bismuthene. In 2005, Nagao *et al.* experimentally elucidated the mechanism of the structural transition of bismuthene layers during their epitaxial growth considering both size and interface effects. According to them, Bi(111) is the favoured plane for thicker films because of the higher cohesive energy compared to Bi(110), which is the opposite for small thicknesses.[52–54] Accordingly, high-quality bismuthene materials with great control of their size and thickness can be synthesized *via* molecular beam epitaxy. This presents an easy option for the synthesis of less defective few-layer bismuthene sheets for various applications.

3.4. Thermal vapour deposition

Thermal vapour deposition is considered to be a cost-effective process for the synthesis of high-quality 2D bismuthene films. Further, considering the low melting point of bismuth (271 °C), this method becomes even more straightforward to prepare 2D bismuthene.[54] In a typical synthesis, the bulk bismuth powder is heated in a furnace under vacuum conditions up to 10 Pa. According to the literature, 2D bismuth with a thickness of 13 nm was prepared by heating Bi powder in a quartz tube furnace at 510 °C with N_2 as the carrier gas at ~1 Pa, leading to continuous large-area Bi(110)-oriented films.[55] However, the large surface roughness of the films, which is highly undesirable, remains the drawback of this method. This can be minimised by oblique angle deposition, which reduces the

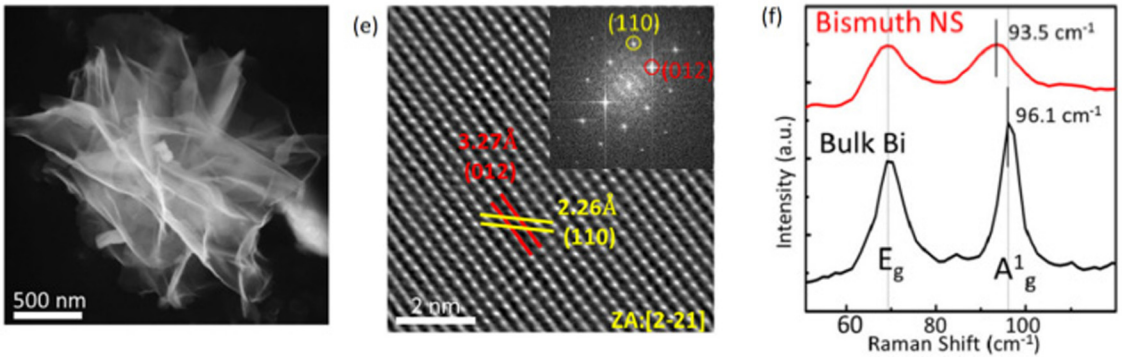

Fig. 5 (a) TEM image, (b) HRTEM image and (c) Raman spectra of bismuthene nanosheets. Reprinted with permission from Wiley.[57]

crystallite size.[56] The sheet-like morphology of bismuthene is shown in Fig. 5 and the peaks in the Raman spectrum of bulk bismuthene shift to a lower value when it converted to nanosheets. The favorable synthesis parameters such as temperature and pressure with high-quality bismuthene sheet yield show that the thermal vapour deposition method can be utilized for the large-scale synthesis of bismuthene sheets for applications in the fields of energy and optoelectronics.

3.5. Magnetron sputtering

The magnetron sputtering process can attain a high deposition rate under a base pressure of 10^{-4}–10^{-5} Pa for the deposition of bismuth thin films with a thickness of hundreds to thousands of nanometers.[54,58,59] This technique produces films with a high surface roughness and is similar to the 2D bismuthene obtained by evaporation and sputtering methods, thus requires optimizations. Recently, Sui *et al.* reported the preparation of bismuth thin films *via* the magnetron sputtering method. In their study on the influence of deposition temperature (from room temperature to near the melting point) on the morphology and structure, they determined that 160 °C is the best temperature to achieve the desired morphology and growth mechanism of bismuthene thin films.[58] Also, compared to the previously reported bismuthene film deposited by magnetron sputtering, segregation was not observed in the films at a substrate temperatures of up to 160 °C, and the authors claimed that it may appear at higher temperatures, such as over 170 °C, as also experimented by Sui and group.[59] However, although magnetron sputtering is a promising method for the synthesis of bismuthene sheets with control of their thickness, the surface roughness and optimization hinder its ability for large-scale synthesis.

3.6. Pulsed laser deposition

This deposition method uses a high energy laser to vaporize and dissociate the material under vacuum, and therefore overcomes the drawbacks of surface roughness obtained *via* the thermal evaporation and sputtering methods by fast moving ions.[60,61] Further, compared with the molecular beam epitaxy method, pulsed laser deposition has the advantages of high deposition rates, low temperature and low cost. However, the synthesis of few-layer or even bilayer 2D-bismuthene has not been reported using this method, limiting its use compared to the epitaxy method.[54] Similar to other deposition methods, the substrate temperature together with the laser (source) energy influences the roughness, grain size and orientation of 2D bismuthene.[60] It has been reported that with a decrease in the substrate temperature, both the grain size and the film roughness also decrease. Thus, by optimizing the deposition parameters, substrate and source energy, 2D bismuthene can be readily deposited in a controlled and desirable manner.[54] However, although the pulsed laser deposition synthesis technique has highly favorable synthesis parameters, it is limited to the synthesis of multilayer bismuth nanosheets, which may not be suitable for several applications.

3.7. Wet-chemical method

Due to its good controllability and high-yield production, wet chemical synthesis is considered to be one of the most potential methods for the preparation of 2D nanomaterials.[62] The synthesis follows simple steps, where initially, the chosen precursor is dissolved in a suitable solvent and treated with reducing agents, followed by the collection of bismuthene by centrifugation, and finally washing. The suitable solvents mostly used are water, glycol, chloroform, thiourea, and ethylenediamine tetraacetic acid disodium.[14,63,64] In most of the reported chemical synthesis methods, the precursors are $Bi(NO_3)_3{\cdot}5H_2O$ and $BiCl_3$. Between them, the nitrate precursor is believed to be a better precursor owing to its high stability under ambient conditions, which also eliminates the undesirable decomposition/degradation. The most popular reported reducing agent is sodium borohydride ($NaBH_4$), which has a few drawbacks, such as its sensitivity to moisture and easy self-hydrolysis. Alternatively, hydrazine has been recently reported to overcome these shortcomings given that it is more stable, water-soluble and can be used in either acidic or basic media.[65] To regulate the growth, shape, and size of the particles and prevent their aggregation, surfactants are added as stabilizing agents. The preparation of bismuthene *via* a surfactant-assisted chemical reduction method was reported, in which the precursor was reduced with a borane-*tert*-butylamine complex in oleylamine (OAm) at 120 °C. In this procedure, OAm acted as

both the surfactant and solvent. Later, the bulk bismuth was exfoliated in various solvents with an ultrasonic probe homogenizer for 1 h to obtain a dark gray suspension of bismuthene nanosheets.[66] In a recent publication, Stefanos *et al.* performed the autoclave-based hydrothermal synthesis of 2D bismuthene with diverse morphologies through the reduction of $Bi(NO_3)_3{\cdot}5H_2O$ by hydrazine at high temperatures and pressure using poly(sodium 4-styrenesulfonate) (PSS) as the surfactant. Using this method, it was reported that at relatively high pressure, the physicochemical properties of the solvents could be controlled by monitoring the solubility and reactivity of the precursors. The autoclave-assisted chemical method also facilitates the production of nanoparticles with the zero-valent state.[65] The reduction of bismuth salt in a solvent using an autoclave is the easiest approach to synthesize bismuthene sheets. The facile synthesis steps make the synthesis of bismuthene easy with great control over the sheet thickness.

3.8. Electrochemical

In almost all the previously reported methods, the scalability of the product remains a major concern. In this case, Osama *et al.*, in their recent work, claimed that the exfoliation of the layered material by the electrochemical method can overcome this drawback.[67] Electrochemical exfoliation is considered a simple and robust technique to efficiently synthesize 2-D nanomaterials with high mass production. Few-layered bismuthene can be prepared using a three-electrode potentiostatic electrochemical station together with cyclic voltammetry (CV) measurements. In a typical experiment, firstly, the bismuth needle is connected to the electrochemical system as the working electrode, and partially placed in the aqueous electrolyte of choice to avoid the contamination of the exfoliated materials, while Pt is used as the counter electrode. The other half cell is made using Ag/AgCl, which acts as the reference electrode to determine the potential of the other half cell. At different applied voltages, exfoliation is performed followed by centrifugation of the electrolyte containing bismuthene as the product (Fig. 6).[67] In a recent publication, Fan *et al.*, for the first time, reported the synthesis of bismuthene nanosheet arrays *via* galvanic replacement reaction. It involves a redox process and the difference in the redox potentials of two metals, leading to the oxidation and dissolution of the metal, and concurrently the reduction and deposition of metal ions from solution. Specifically, the galvanic replacement reaction between metallic Cu and Bi^{3+} ions was performed for the development of densely and vertically aligned bismuthene nanosheet arrays on Cu substrates.[68] Further, recently, 2D mosaic Bi nanosheets with a mosaic morphology were created by electrochemically reducing bismuth oxyiodide (BiOI) nanosheets *in situ*. Nanoflakes with a size of about 10 nm developed and were distributed throughout the matrix of the Bi nanosheets.[69] The results show that electrochemical exfoliation is a facile and reliable technique for the synthesis of few-layer bismuthene, which can be implemented in various applications, as explained in the next section.

The large-scale synthesis of defect-free few layer bismuthene nanosheets is still a challenge due to their susceptibility to oxidation, sensitivity to impurities, and limited availability of starting materials. Moreover, the methods for the synthesis of other 2D materials cannot be directly applied to bismuthene due to its unique structure and properties. Thus, researchers are still exploring the possibility of realizing the large-scale synthesis of bismuthene.[70] Although the synthesis of bismuthene is challenging, other analogues of bismuth such as three-dimensional bismuth nanoparticles and bismuth nanorods are easy to synthesize, even on a large scale. Currently, bismuth nanoparticles are being applied in biomedical research due to their biocompatibility and antibacterial property. Generally, bismuth nanoparticles are synthesized though the reduction method using appropriate reducing agents such as sodium borohydride or hydrazine.[71–73] This method produces small and uniform nanoparticles, but it requires careful control of the reaction conditions to avoid agglomeration and oxidation. As reported by Wu *et al.*, the solvothermal synthesis method also can be implemented for the synthesis of bismuth nanoparticles.[74]

Another type of bismuth analogue, bismuth nanorods, can be synthesized through the chemical reduction method. Bismuth nanorods with an average diameter of 30 nm and 100–1000 nm in length were synthesized by Petsom *et al.* by reducing bismuth nitrate in the presence of hydrazine hydrate.[75] Similarly, Long *et al.* also followed the solvothermal method and *in situ*

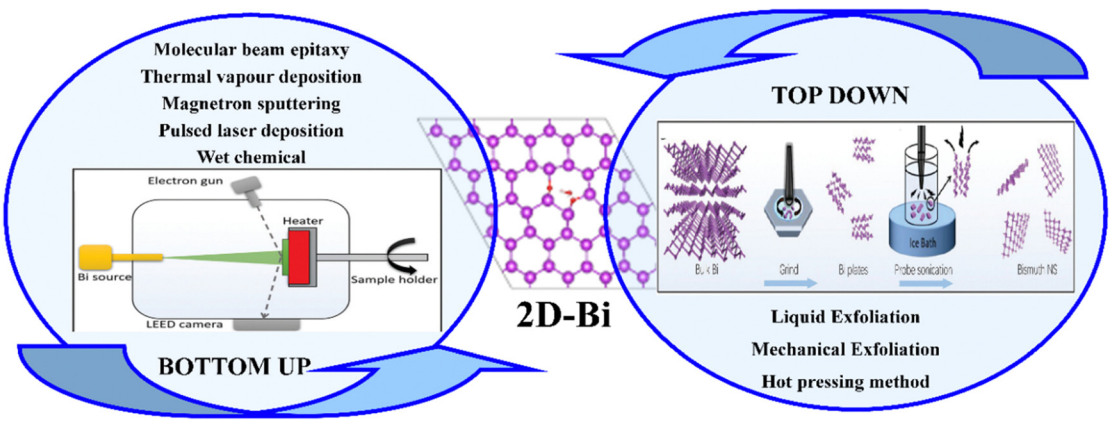

Fig. 6 Schematic representation of the different techniques for the synthesis of monoelemental bismuthine.

thermal reduction method to obtain bismuth nanorods confined in doped carbon nanotubes for battery applications.[76] Besides bismuth nanoparticles and nanorods, there are also a few reports on bismuth nanoribbons,[77] bismuth dots[48,78] and bismuth nanoplates[79] synthesized through techniques such as the sol–gel method, chemical reduction method and microwave-assisted synthesis method. Bismuth particles, irrespective of their dimensions, manifest unique physical, optical and electrical properties, which with some modifications can be adopted in various fields especially in the field of biomedicine.

In conclusion, the various techniques used to synthesize 2D bismuthene have their advantages and drawbacks. Among the discussed methods, the common methods used for the synthesis of bismuthene include mechanical exfoliation, chemical vapor deposition (CVD), and molecular beam epitaxy. Although the methods to prepare 2D bismuthene offer several advantages, they also have some drawbacks, which can limit their applicability. Here, we present some solutions to overcome the limitations of these methods. Chemical vapor deposition requires high temperatures and a controlled gas flow, which can limit its scalability and reproducibility. One solution is to use low-temperature CVD, which involves using plasma to activate the precursor gas and reduce the required temperature. Another solution is to use aerosol-assisted CVD, which involves dispersing the precursor gas in an aerosol to improve the uniformity and reduce the generation of defects. Molecular beam epitaxy requires ultrahigh vacuum conditions and a high level of control over the deposition process, which can limit its scalability and throughput. One solution is to use a hybrid MBE/CVD approach, which combines the precision of MBE with the scalability of CVD. Another solution is to use a pulsed laser deposition method, which can deposit bismuthene at high rates with good crystalline quality. Alternatively, the electrochemical deposition can be slow and require complex electrode designs, which can limit its scalability and reproducibility. One solution is to use a modified electrochemical deposition method that involves adding surfactants or additives to the solution to improve the deposition rate and quality. Another solution is to use a template-assisted electrochemical deposition method, which involves using a nanoporous template to guide the deposition and improve the uniformity. Further, liquid-phase exfoliation can produce bismuthene with variable thickness and quality, which can limit its reproducibility and scalability. One solution is to use a surfactant-assisted liquid-phase exfoliation method, which involves adding surfactants to the solvent to improve the exfoliation yield and quality. Another solution is to use a bottom-up synthesis method, such as CVD or MBE, to produce high-quality bismuthene, and then use exfoliation to produce thinner layers.

Given that each of these techniques has its advantages and drawbacks, the choice of method will depend on the specific application and the desired properties of the synthesized bismuthene. Overall, the drawbacks of the methods to prepare 2D bismuthene can be addressed through a combination of process optimization, innovative approaches, and the development of new techniques. Researchers are actively working to overcome these challenges and improve the methods for the synthesis of bismuthene to achieve high-quality, large-area, and uniform samples.[21,32,80,81]

4. Applications

4.1. Electrochemical and photocatalytic applications

Bismuthene with a large number of surface active sites and high surface area due to its 2-dimensional sheet-like structure can be a very efficient catalyst for electrochemical and photocatalytic reactions. Hence, researchers are now trying to implement bismuthene/its composites in various electrochemical and photochemical applications such as electrochemical hydrogen evolution, electrochemical sensing, electrochemical and photocatalytic CO_2 reduction. An efficient catalyst with a low overpotential, high current density and long-term stability is needed for the large-scale and efficient production of green hydrogen. In this regard, electrochemical hydrogen evolution studies using bismuth nanosheets were carried out by Duan *et al.* Bismuth nanosheets were synthesized through the liquid-phase exfoliation method assisted by sonication. The nanosheets showed an overpotential value of −958 mV at a current density of 10 mA cm^{-2} and the Tafel slope value of 122 mV dec^{-1}, which are much higher compared to that of their bulk counterpart. The higher activity observed is due to the higher number of active sites present across the edges of the 2D structure.[82] Lazanas and co-researchers[42] synthesized bismuthene through the method of shear-force liquid-phase exfoliation for the hypersensitive stripping voltammetric determination of cadmium ions and lead ions though electrochemical sensing (Fig. 8a). A bismuthene dispersion was combined with few layers of graphene and coated on a glassy carbon working electrode. Graphene acted as the supporting material to attain the required adherence of bismuthene films. With Ag/AgCl as the reference electrode and platinum as the counter electrode, they achieved a limit of detection of 0.3 mg L^{-1} for both lead and cadmium in the presence of potassium hexacyanoferrate(II) in tap water samples. Tapia *et al.* synthesized few-layer bismuthene through shear force exfoliation for the electrochemical sensing of cadmium and lead. A bismuthene carbon-based screen-printed electrode was devised by drop-casting the exfoliated bismuth suspension on a screen-printed carbon electrode as the working electrode surface. This electrode was utilized for the electrochemical detection of lead and cadmium. Due to its excellent mobility, high surface area and high number of active sites, they achieved a limit of detection of 0.06 μg L^{-1} and 0.07 μg L^{-1} for lead and cadmium ions, respectively, in aqueous samples.[83] Isa *et al.*[84] studied the adsorption of CO, SO, CO_2, SO_2, H_2S and NH_3 gases on silver-decorated buckled bismuthene (b-Bi) through DFT. According to this study, gases contributed to improving the electronic properties of Ag-*b*-Bi due to the hybridization of Ag-*b*-Bi with gases and charge transfer between them. Additionally, Ag-*b*-Bi also shows stability against humidity.

Panigrahi *et al.*[85] performed a DFT study on pristine and defect-crafted bismuthene (bBi) sheets for the sensing of nitrogen-rich and sulfur-rich (NH_3, NO_2, H_2S, and SO_2) toxic gases. This study suggested that bBi shows higher and selective gas sensing towards NO_2 molecules compared to other gases, which is attributed to the substantial charge redistribution and stronger adsorption energies. Additionally, mono- and di-vacancy-induced bBi sheets have improved sensitivity, which is ascribed to the modification in the electrostatic potential difference between the gas molecules and bismuthene sheets (Fig. 7a). In a more recent study, calculations using density functional theory (DFT) were utilised to examine the effects of anchoring and doping on the gas detection capability of bismuthene as a substrate material. It was discovered that surface structure modifications using single metal atoms (Ba, Be, Ca, K, Li, Mg, Na, and Sr) can help to increase its sensitivity for gas detection. Bismuthene (bBi) in a buckled honeycomb structure with the Be atom anchored (A-Be-Bi) demonstrated enhanced H_2S sensitivity.[87] Zhang *et al.*[86] prepared atomically thin bismuthene and studied its performance for the electrochemical sensing of Cd^{2+} and Pb^{2+} both simultaneously and individually. The synthesized bismuthene exhibited high sensitivity and anti-interference ability. DFT studies revealed that Bi-ene shows excellent adsorption capacity for Pb and Cd in comparison to Bi-nanosheets due to the lower adsorption energy for the Pb^{2+} ion (−3.43 eV) and Cd^{2+} ion (−0.71 eV) in Bi-ene(111) than in Bi-nanosheets (001), as shown in Fig. 7(b–e). Snehha *et al.*[88] studied bismuthene nanotubes as a chemiresistor sensor through a first principle study for sensing NO_2, PH_3, and NH_3 gas molecules and revealed that upon adsorption, charge transfer occurs between the gas molecules and bismuthene nanotubes.

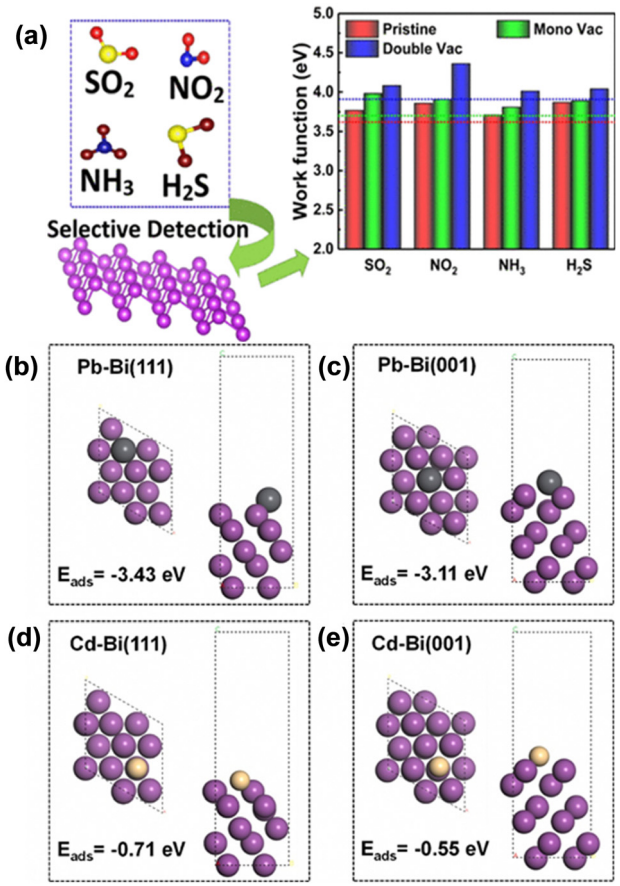

Fig. 7 (a) Sensing of SO_2, NO_2, NH_3, and H_2S gas using bismuthene. Reprinted with permission from ACS.[85] Adsorption energies and adsorption configurations of lead on (b) Bi-ene and bismuth nanosheets (c) and cadmium on Bi-ene (d) and (e) bismuth nanosheets, respectively (black, yellow and violet balls represent Pb, Cd and Bi atoms, respectively). Reprinted with permission from Elsevier.[86]

Bismuthene can also be employed for the CO_2 reduction process. Cao *et al.* synthesized bismuthene sheets with a thickness ranging from 1.28–1.45 nm from ultrathin bismuth-based metal–organic layers through an *in situ* electrochemical transformation process. The as-synthesized bismuthene was applied for electrochemical CO_2 reduction. The bismuthene sheets showed high selectivity, high intrinsic activity and nearly 100% faradaic efficiency for formate production with long-time stability and exceptional partial current density. The researchers with a self-designed flow cell could achieve current densities larger than 300 mA cm^{-2} for formate production, as presented in Fig. 8b.[89] Yang and co-researchers synthesized free-standing 2D bismuth nanosheets having various thickness through a reduction reaction. Density function theory calculation showed the easy and selective formation of $HCOO^-$ on the bismuthene(111) facet due to its distinctive compressive strain. The synthesized material was applied for the electrochemical CO_2 reduction reaction and found high faradaic efficiency of 99% at −580 mV, durability of >75 h and small onset overpotential of <90 mV.[18] Ning *et al.* engineered atomically thin bismuth nanosheets from a Bi_2O_2S precursor with rich and stabilized Bi–O bonds for the electrochemical conversion of carbon dioxide into formate.[63] They observed a cathodic energy efficiency of >60% and high Faraday efficiency of >90% in the wide current density range of 50 to 400 mA cm^{-2} to produce formate. This enhanced performance is due to the large number of Bi–O bonds, which enhanced the CO_2 adsorption on the catalyst surface (Fig. 8c). Fan *et al.* synthesized bismuthene nanosheet arrays with a large area and vertically aligned structure, which were grown on a copper substrate *via* galvanic replacement reaction. The nanosheets were found to have small thickness of about 2–3 atomic layers, abundant porosity, high stability and large surface area. The synthesized nanosheets were applied for the electrochemical reduction of CO_2 to formate, which showed high selectivity of more than 90% and large partial current density of 45 mA cm^{-2}.[90] He *et al.* prepared an integrated 3D open network of interconnected bismuth nanosheet arrays through *in situ* electrochemically topotactic transformation. The obtained 2D atomically thin bismuthene integrated array superstructure had desirable properties including remarkable intrinsic activity, high number of active sites, and superior mass and charge transfer capability. The electrochemical CO_2 reduction reaction was studied, as shown in Fig. 8d, and steady formate production with a large faradaic efficiency of about 90% and current density of >300 mA cm^{-2}

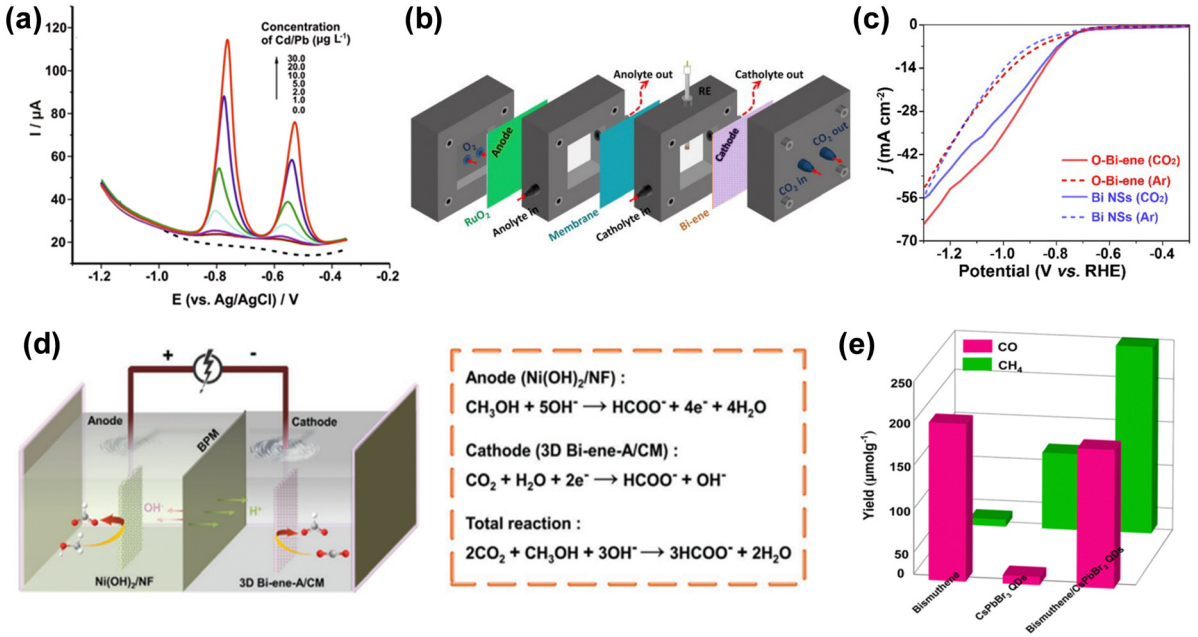

Fig. 8 (a) Square-wave stripping voltammograms of 1 : 5 bismuthene:graphene-modified electrode with Pb ions and Cd ions. Reprinted with permission from Elsevier.[42] (b) Schematic diagram of the electrocatalytic CO_2 reduction reaction self-designed flow cell. Reprinted with permission from Wiley.[89] (c) Polarization curves of electrochemical CO_2 reduction reaction. Reprinted with permission from Elsevier.[63] (d) Schematic diagram and electrochemical reactions of two-electrode electrolyzer for electrocatalytic CO_2 reduction reaction/methanol oxidation reaction. Reprinted with permission from Wiley.[91] (e) Total CO_2 photoreduction yields of bismuthene, $CsPbBr_3$ QDs, and bismuthene/$CsPbBr_3$ QDs. Reprinted with permission from ACS Publications.[93]

was achieved with long-term stability, prominent selectivity and high formate partial current density.[91] A 3D porous electrocatalytic membrane with conductive network was assembled from atomically thin bismuthene nanolayers with rich edge-site defects by Zhang *et al.*[92] These efficient super-structured electrocatalytic membranes were employed for the conversion of CO_2 to formate, achieving a current density of up to 560 mA cm^{-2} with continuous operation for more than 500 h at a high current density without any major decay in activity because of the presence of active sites with high intrinsic activity, high conductivity and multiple interconnected channels in the material. A bismuthene and $CsPbBr_3$ quantum dot S-scheme heterojunction was constructed by Min Zhang and team for photocatalytic CO_2 reduction. The heterojunction was synthesized through an *in situ* growth method. Under UV-visible light irradiation and without any sacrificial agents, the material exhibited improved photocatalytic performance with a yield of 157.76 μmol g^{-1} and 215.56 μmol g^{-1} for CO and CH_4, respectively, as shown graphically in Fig. 8e.[93] Zhu *et al.*[94] prepared bismuth quantum dots and applied them for photodetector application, which showed a photocurrent density of 2690 mA cm^{-2} and photoresponsivity of 22.0 μA W^{-1} due to their suitable band gap and accessible active sites. Gong *et al.*[81] developed a bismuthene@MXene ($Ti_3C_2T_x$) heterostructure for capacitive deionization, which showed high desalination capacity (88.2 mg g^{-1} at 1.2 V). This heterostructure exhibited a large number of active sites together with ion and electron transport as well as provide strong interfacial interaction between bismuthene and MXene. The research on 2D monoelemental bismuthene is in its infancy, and thus this material is not widely explored to date. Nevertheless, due to its unique band structure, electrical properties and high number of surface active sites, bismuthene can be a key material for electrochemical and photocatalytic applications.

4.2. Optoelectronic applications

Researchers are also trying to implement bismuthene in electronic and optoelectronic applications due to its thin structure and unique semiconducting properties. Basyouni and co-researchers prepared few-layer bismuthene as a reverse saturable absorber material through the electrochemical exfoliation of bismuth. The few-layer bismuthene showed a wide absorption and PL response range from the UV to IR region due to the confinement effects and crystal dislocations or defects, which shows the potential of few-layer bismuthene as a new optical material for ultrafast photonic applications such as optical limiters.[21] Zhong *et al.* grew 2D bismuth samples ($\leq$30 nm) on an Si(111) substrate *via* molecular beam epitaxy.[95] The researchers found that the electrical conductivity, thermal conductivity and Seebeck coefficient of 2D bismuth were measured up to 46250 S m^{-1}, 1.25 W m^{-1} K^{-1} and −237 μV K^{-1} at room temperature, respectively. The results shed light on the potential applications of bismuthene in electronic devices. Few-layer bismuthene nanosheets synthesized through liquid-phase exfoliation and coated on a K9 glass substrate were used as a saturable absorber by Chen *et al.* The shortest pulse width of 361 ns and the maximum absorbed pump power of 3.55 W were achieved with the peak power 1.52 W and the

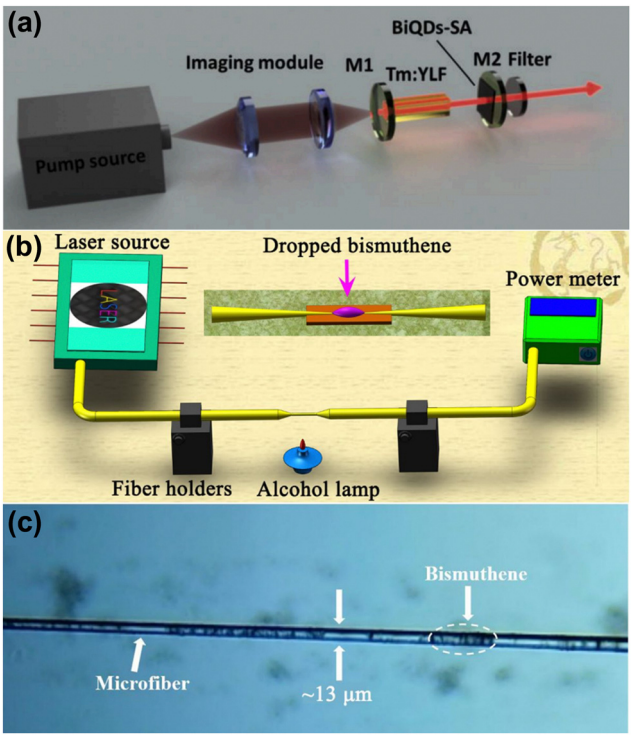

Fig. 9 (a) Schematic of Q-switched laser cavity based on bismuthene quantum dots. Reprinted with permission from Elsevier.[78] (b) Schematic diagram of the experimental setup for the fabrication of a microfiber. Reprinted with permission from ACS Publications.[96] (c) Microscopy image of the prepared microfiber saturable absorber based on bismuthene. Reprinted with permission from ACS Publications.[96]

repetition rate of 365 kHz.[4] Pan *et al.* synthesized bismuthene quantum dots through liquid-phase exfoliation, which were transferred to a quartz substrate and applied as a saturable absorber in a Tm:YLF laser (Fig. 9a) operating at 2 μm due to their broadband absorption property. The minimum pulse width and the repetition rate achieved were 440 ns and 94 kHz, respectively, with a peak power of 8.1 W and maximum single pulse energy of 4.5 μJ.[78] Dong *et al.* synthesized bismuthene quantum dots *via* the liquid-phase exfoliation method, which were applied in a near infrared pulsed laser as a saturable absorber.[48] These researchers achieved a repetition rate of 457 kHz and pulse duration of 155 ns at 1.34 μm. Feng *et al.* studied bismuthene nanosheets and their nonlinear optical properties, which were applied in a passively mode-locked fiber laser. The researchers deposited the bismuthene nanosheets on microfibers to make a saturable absorber, as shown in Fig. 9b and c and achieved the modulation depth and the saturation intensity of 1% and 2.4 MW cm^{-2}, respectively.[96] The saturable absorption property of exfoliated few-layer bismuthene was also studied by Guo *et al.* with the saturable intensity of 110 MW cm^{-2} and modulation depth of 2.5% at the optical communication band.[97] Maheshwaran *et al.*[98] reported the preparation of a bismuthene-graphitic carbon nitride (Bi-g-C_3N_4) composite as a supercapacitor, and then integrated it with dye sensitized solar cells (DSSC) consisting of TiO_2/N719 dye as the electron transport layer and sensitizer, respectively. Bi-g-C_3N_4 as the cathode showed an energy density of 31.597 μW h cm^{-2} with a power density of 3.25 MW cm^{-2} and the integrated DSSC exhibited an energy storage efficiency of 68.35%. Xue *et al.*[99] prepared a bismuthene-SnO_2 heterojunction and studied it as an electron transport material in perovskite solar cells. This heterojunction exhibited an upshifted energy band gap and reduced interfacial resistance between perovskite and the composite material, resulting improved electron extraction. Bismuthene-SiO_2 showed a power conversion efficiency of 18.75%. The bandgap, wide UV-visible range absorption and low mass of bismuthene make it a suitable material for optoelectronic applications. Due to its structure and properties, bismuthene can be a revolutionary material as a saturable absorber. Topological insulators exhibit attractive physical properties, which are promising for spintronics applications. Bismuthene has attracted attention due to its large nontrivial gap due to the strong spin orbit coupling of Bi and unusual strong interaction between Bi atoms and surface atoms of the substrate. In this case, Liu *et al.*[100] prepared bismuthene on GaAs, which possessed a large Bi–As binding energy, and as expect bismuthene, induced an electronic band in the band gap of GaAs, opening a gap that has a nontrivial topological nature. Abdelfatah *et al.*[101] doped the p-type dopant tetrafluoro-tetracyanoquinodimethane (F4TCNQ) in bismuthene to achieve surface charge transfer. The doped bismuthene showed a carrier lifetime of 6.5 μs after doping, suggesting enhanced p-type conductivity, which is ascribed to the unusual charge transfer interaction between bismuthene and the F4TCNQ molecules. Bismuthene quantum dots with an average diameter of 26 nm were synthesized by Pan *et al.*[102] through the solvothermal synthesis method. A saturable absorber was prepared using bismuthene quantum dots with excellent saturable absorption properties with a maximum modulation depth of 5.1% at 1.5 μm due to the quantum effect caused by their ultra-small size. Further, the passive mode locking operation was carried out in an erbium-doped fiber laser with bismuthene quantum dots, which generated conventional soliton pulses and dissipative soliton pulses with a duration of 835 fs and 575 fs at the repetition rate of 9.23 MHz and 7.83 MHz, respectively. The results manifest the potential of bismuthene quantum dots as an optical modulation device for ultrafast lasers. The bandgap, wide UV-visible range absorption and low mass of bismuthene make it a suitable material for optoelectronic applications. Due to its structure and properties, bismuthene can be a new material as a saturable absorber.

4.3. Supercapacitors

Due to their high power density (104 W kg^{-1}), quick charge-discharge speed, great cyclic stability (10^6 cycles), and low equivalent series resistance, supercapacitors (SC) are regarded as potential energy storage technology.[103] However, their unsatisfactory energy densities limit their practical applications, and thus to address the rising need for energy, research has been devoted to investigating sustainable, affordable, and efficient energy storage solutions.[104] Owning to the exceptional

electrochemical activity of ultrathin, layered 2D metallenes, they have become a hot research topic to improve energy storage applications. Particularly, due to their unique characteristics, such as their tunable band-gap (0.18 to 2.6 eV), enhanced carrier motilities, high surface area, adaptable interlayer gap, superior mechanical stability, and exceptional adjustability of the atomically thin monolayer sheets, bismuthene has caught the attention of researchers.[103] Researchers have demonstrated that 2D bismuthene can serve as a potential substitute electrode for prospective energy storage systems, particularly supercapacitors and the same has been reviewed in this section. The gravimetric capacity of the bismuthene nanosheets at 10 mV s^{-1} was determined by cyclic voltammetry analysis, and the findings were assessed. Additionally, employing bismuthene/activated carbon (AC), the asymmetric supercapacitor achieved the maximum specific capacity of 87.3 mA h g^{-1} at 1 A g^{-1}, with an energy density of 27.23 W h kg^{-1} and power density of 312.5 W kg^{-1}.[103] The fabrication of bismuthene-graphene with a hierarchical 3D microstructure as both the negative and positive electrode was studied by Wei *et al.*, which showed a specific capacitance of 400.83 F g^{-1} at 0.67 A g^{-1}. The energy density of 45.55 W h kg^{-1} at 400 W kg^{-1}, together with the cycling stability of 89.24% after 3600 cycles was reported. The incorporation of conductive bismuthene flakes in the porous graphene aerogel framework enhanced the electron/ion transfer due to the dual transport channel design. This resulted in the extension of the space between the layers and an increase in the conductivity to facilitate the electron transport, enhancing the overall performance of the electrochemical device to store energy.[105] Bismuth nanosheets were assembled in all-solid-state supercapacitors and the device exhibited a volumetric capacitance of 36.8 F cm^3 with notable volumetric energy and power densities. It was observed that by compositing them with carbon nanotubes (CNTs), the volumetric capacity was enhanced by up to 68.7 F cm^3. The highest possible volumetric power and energy densities were 203.2 W cm^3 and 9.5 mW h cm^3, respectively. The authors also noted that the Bi/CNT devices demonstrated high flexibility with about 79.0% preservation of the initial capacitance and greater cycling stability with 82.2% preservation of the initial capacitance after 20 000 cycles, highlighting the great potential of Bi/CNTs for high-performance flexible solid-state supercapacitors, as shown in Fig. 10.[106]

The notable electrochemical performance was attributed to their high conductivity, high surface area, porous structure, and good electrode/electrolyte contact, which synergistically enhanced the overall performance of the supercapacitor. It was observed that the stability and high energy density could be improved by modifying the structure of the nanomaterials. Thus, the reported stability and performance of the newly developed bismuth yttrium oxide material may be potentially used for practical purposes to enhance the productivity of storage devices.[107] The high energy density and specific capacitance values found in the early research on bismuthene due to its properties such as tunable bandgap, high surface area, carrier motility and stability suggest that the bismuthene nanosheets are promising materials for supercapacitor application in the near future.

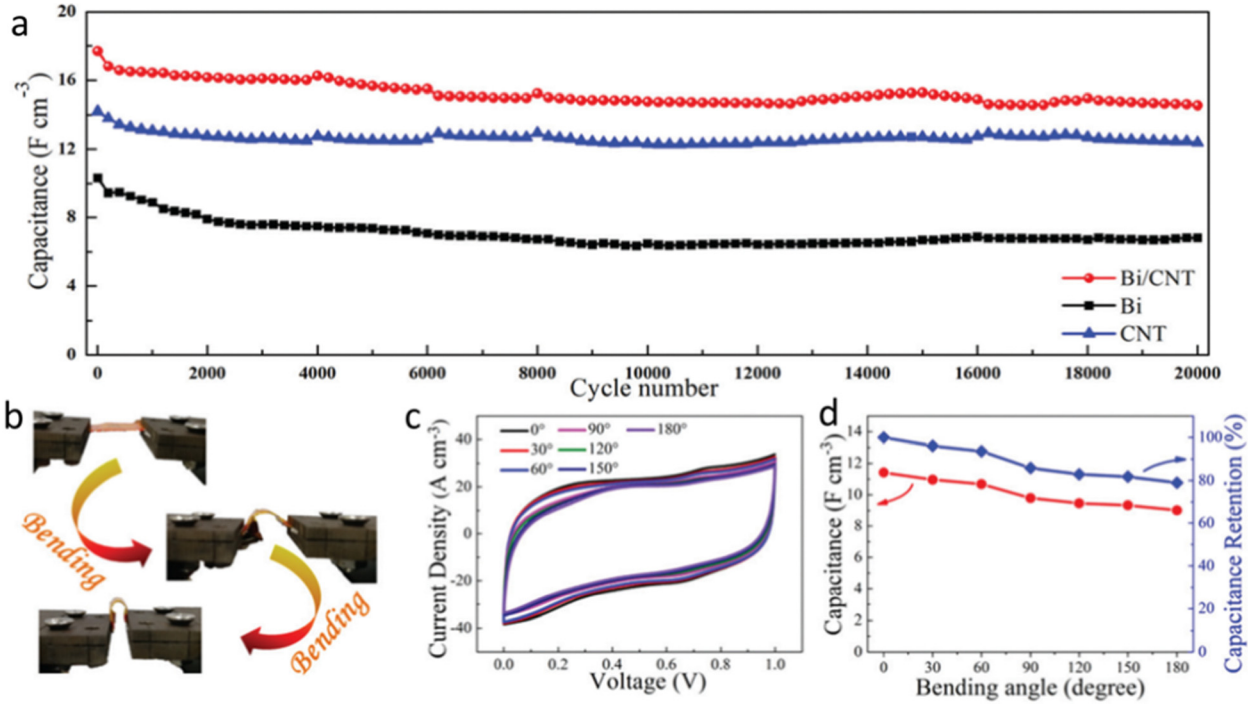

Fig. 10 (a) Cycling performance of capacitance for Bi/CNTs, Bi and CNTs at a scan rate of 0.5 V s^{-1}. (b) Photographs of Bi/CNTs tested under different bending angles. (c) CV curves obtained at different bending angles, at 0.5 V s^{-1}. (d) Volumetric capacitance and capacitance retention as a function of bending angle. Reprinted with permission from RSC.[106]

4.4. Batteries

Bismuthene shows a high theoretical volumetric capacity, high carrier mobility, moderate layer distances and low working potential, which are ideal characteristics for an anode material, and hence it has been studied as a promising anode material for batteries. Khan *et al.* performed first principle calculations for buckled bismuthene (b-Bi) as an anode material for Li/Na batteries. The theoretical studies suggested high storage capacities of 2276 mA h g^{-1} and 2149 mA h g^{-1} for Li and Na, respectively (1896 mA h g^{-1} for K). Additionally, the adsorption energies for Li, Na and K found to be −2.7 eV, −2.9 eV and −3.45 eV, respectively, which indicate their good stability. The sodiation mechanism in bismuthene studied through *in situ* TEM revealed a multistep crystal phase evolution with Bi-NaBi-Na_3Bi associated with a large anisotropic volume expansion of 142% along the *z*-axis. Na_3Bi has a gravimetric capacity of 385 mA h g^{-1} and elemental Bi exhibits a high volumetric value of 3800 mA h cm^{-3}. The reaction between Na and Bi is typically an alloying process (Fig. 11).

Wang *et al.*[109] theoretically studied a bismuthene/graphene heterostructure anode for Li-ion batteries (LIBs). The monolayer β-Bi has a stiffness of 33.0 N m^{-1}, whereas the Bi/G heterostructure showed higher stiffness of 369.2 N m^{-1} with improved electrical conductivity, thermal and mechanical stability. Additionally, the diffusion barrier of 0.32 eV and volume expansion ratio of only 4% ensured rapid Li^+ ion transport in the charge/discharge cycling process and long life of the LIB. Xu *et al.*[110] integrated bismuthene in poly(ethylene oxide) (PEO) electrolyte in Li batteries, which showed enhanced ionic conductivity because of the weakened bond strength of O (-EO) and Li^+, destruction of the crystal structure of PEO and greater mobility. Also, the addition bismuthene reduced the diffusion barrier of Li^+ and the in situ-formed LixBi-rich layer stabilizes the Li/PEO interface and restricts the formation of lithium dendrites. The Bi/PEO composite electrolyte showed stable cycling for 1000 h with a current density of 0.2 mA cm^{-2} in an Li symmetric battery. Zhou *et al.* discovered that ultrathin bismuthene with a high aspect ratio could relieve the anisotropic volume expansion produced by the alloy reaction during the process of sodiation. Free standing bismuthene-graphene films in an Na-ion battery showed a reversible capacity of 317 mA h g^{-1} after 1000 cycles at a current density of 1.2 mA cm^{-2}.[111] A multifunctional piezo-electrolyte-based nanogenerator was fabricated by Maheshwaran *et al.*[112] using two-dimensional bismuthene-hexagonal boron nitride nanocomposite as the cathode, activated carbon as the anode and polyvinyl alcohol–potassium hydroxide–barium titanate as the piezo-electrolyte. Bismuthene was synthesized through the liquid-phase exfoliation method. The fabricated device delivered a specific capacity of 280 C g^{-1} at 1 A g^{-1} with high power density and energy density values of 11250 W kg^{-1} and 87.5 W h kg^{-1}, respectively. Through thumb impact, the practical utilization test was conducted on the device, which displayed the self-charging of 146 mV. This demonstrates a new way for the development of smart devices. The experimental results, which are also backed by theoretical studies, reveal the potential of bismuthene nanosheets and direct the attention towards the efficient use of bismuth nanosheets as anode materials in batteries.

4.5. Biomedical applications

Due to their many advantages, such as non-toxic nature, low-cost, high biocompatibility, broadband absorption and good X-ray attenuation property, bismuth-based materials have attracted attention from researchers for versatile biomedical applications such as in bio-imaging, therapeutics, biosensors, and antibacterial. Bi nanoparticles are employed as photothermal therapy, image-guided X-ray radiation, and contrast agents in computed tomography (CT) imaging, and thus are considered to be highly efficient targeted agents for cancer treatment. They provide a novel interesting platform for combination image-guided photoradiotherapy to be widely used in biomedical applications (Fig. 12). Bulmahn *et al.* reported that laser-synthesized elemental Bi nanoparticles with a vanishing band

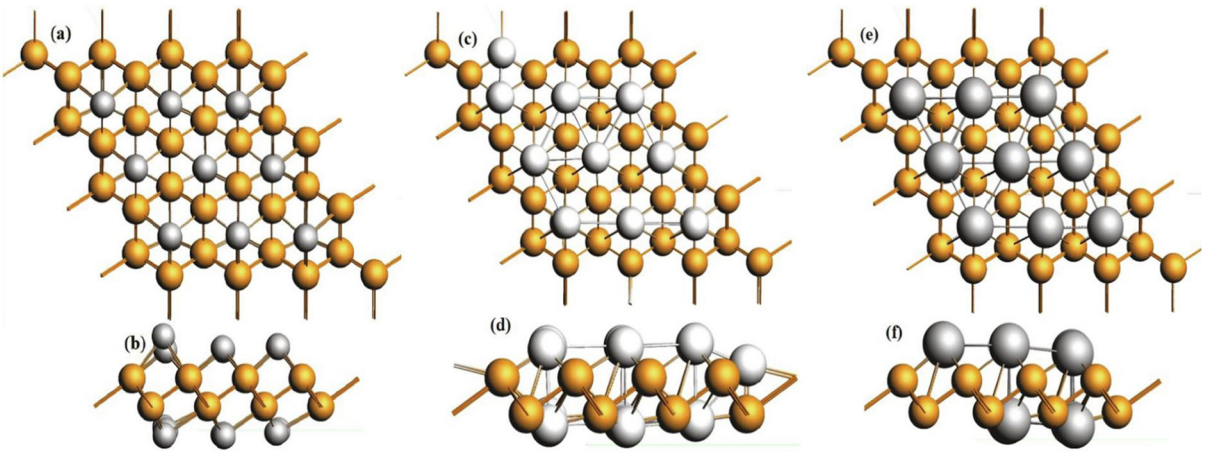

Fig. 11 Fully lithiated, sodiated and potassiated b-Bi structures from *z*-axis (a, c and e) and *x*-axis (b, d and f) views, respectively. Reprinted with permission from Elsevier.[108]

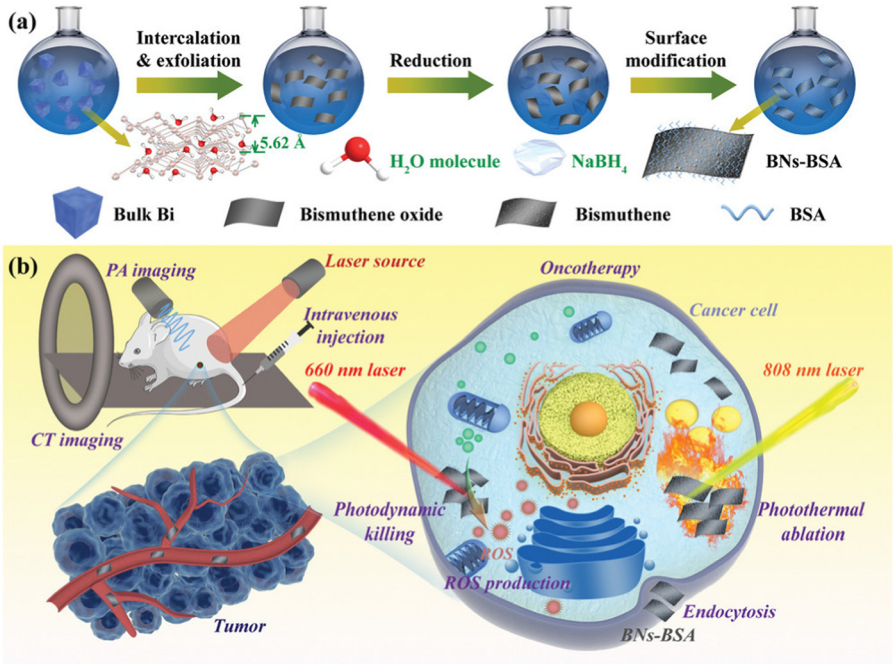

Fig. 12 (a) Schematic representation of bismuthene surface modification and (b) biomedical application in cancer treatment. Reprinted with permission from Wiley.[2]

gap exhibited notable absorption in the infrared range, activating photothermal therapy with maximum optical transparency in biological media.[34,113,114] High Z elements such as iodine and bismuth are preferred in a variety of X-ray imaging techniques due to their superior and substantially less expensive X-ray attenuation performance compared to standard CT agents. The edge value of bismuth is three-times that of iodine-based medicine (K = 33.2 keV), which has better imaging potential and a marginally higher X-ray absorption efficiency. Ultra-small PVP-coated Bi nanodots were prepared by Lei *et al.*, wherein they observed that the resolution of the CT imaging is three-times higher than that of the conventional iodine-based contrast agent.[34] Further, Liu *et al.* prepared Bi@gelatine nanoparticles and their study revealed an enhanced CT signal and excellent CT imaging. Bi-based nanomaterials are viewed in this regard as a potential substitute for *in vitro* and *in vivo* imaging.[115] Also, the immune-cytochemistry process was performed to investigate the targeting ability of hyaluronic acid (HA)-coated ultrasmall BiOI nanoparticles on human colon cancer cells with the CD44 antigen. It was determined that at comparable concentrations, X-ray attenuation was higher than iohexol, a commercially produced iodinated contrast agent, which can be administered at considerably lower doses to provide equivalent contrast.[116]

A bismuthene/bismuth oxide (Bi/BiOx)-based nano-heterostructure, upon irradiation at 660 nm, was reported to synergistically enhance photo-dynamic therapy (PDT) by improving tumor tissue penetration and increased cellular uptake, which provided better oxygen-independent tumor ablation with 660 nm irradiation compared to traditional PDT agents.[117] Further, recently, Ying *et al.* reported combined applications including photothermal, photocatalytic and chemotherapy for cancer treatment using bismuthene nanosheets for the first time. The (polyethylene glycol) PEG-modified partially oxidized bismuthene nanosheets were used as a drug delivery agent with the antitumor drug doxorubicin. The material showed photothermal treatment ability under near infrared light, which promoted the cellular uptake of the drug. More importantly, it was observed that through photocatalytic pathways under red light irradiation, it was able to reduce CO_2 to CO in cancer cells. The CO that is produced is known to lessen tumour cell drug resistance brought on by chemotherapy and the inflammation that results from photothermal therapy. Consequently, the multipurpose bismuthene nanosheets have strong therapeutic potential because they not only had a significant anticancer impact but also minimal adverse effects.[118] Furthermore, merging various imaging methods can possibly enhance the spatial and temporary sensitivity of imaging systems for tumor therapy. The targeted therapy used for the treatment of the disease is vital in clinical medicine. Chemotherapy, photothermal therapy (PTT) and photodynamic therapy (PDT) are the most common therapies, which can be improved based on the modification of nanostructures. Due to the unique optical performance of bismuthene, which exhibits strong absorption in the region of near infrared light, it is widely used as a photothermal agent for PTT. In 2020, Liu *et al.* reported for the first time the biomolecule-directed synthesis of Bi nanoparticles for biomedical applications.[119,120] A better photothermal conversion potential under 808 nm laser irradiation and at the power of 1.3 W cm^{-2} was reported to be observed using (polyvinyl pyrrolidone) PVP-encapsulated Bi quantum dots (PVP-Bi QDs) with the photothermal conversion efficiency of

about 30% with negligible cytotoxicity effects on normal cells.[121] Chai *et al.* engineered a biomimetic *in situ* oxygen-evolving platform with 2D bismuthene as the radio-sensitizing agent, which successfully introduced microbial therapy in tumor radiotherapy.[20] By converting H_2O_2 into $^{\bullet}OH$, the oxidation of Bi^0 to Bi^{3+} initiated chemodynamic treatment (CDT). The Bi-DMSN@PCM nanosystem, which was created by the *in situ* growth of Bi nanodots with a coating of phase-change material (PCM) on the surface of dendritic mesoporous silica nanoparticles (DMSNs), was exposed to low power density near infrared-II laser radiation. The heat produced by the Bi nanodots caused the PCM shell to melt, triggering CDT and heat-induced photothermal therapy (PTT).[122] Recently, Xue *et al.* developed an ultrathin bismuthene-based sensing platform (Fig. 13a–c) for the quantitative and specific detection of microRNA (miRNA), capable of discriminating even single-base mismatches with a detection limit of up to 60 pM. They further explored the quenching mechanism of bismuthene fundamentally by performing intracellular experiments. Consequently, their study revealed that the dye-labeled ssDNA probe could be absorbed on the surface of bismuthene nanosheets due to the van der Waals force between the nucleobases and the basal plane of bismuthene. Bismuthene was observed to efficiently quench the dye-labeled ssDNA, and thus showed an outstanding quenching. However, the target miRNA led to fluorescence recovery, which was primarily due to the corresponding binding between dye-ssDNA and the target miRNA-21, and then desorption from the bismuthene nanosheets, as also depicted in Fig. 13(d–g).[15] The biocompatibility of bismuthene nanosheets makes them very suitable materials for biomedical applications. We have barely explored the capabilities of bismuthene nanosheets in the field of cancer treatment and bio imaging to date, which can develop into a prominent material for biomedical applications in the future.

Varzandeh *et al.*[123] synthesized thioglycolic acid-modified bismuth nanosheets through sonication as a remotely controlled radio-sensitizing, drug delivery, and photothermal therapy agent. The bismuthene nanosheets were found to be 1–3 atomic layer thick with a thickness of around 40–60 nm. The thioglycolic acid functionalization of bismuthene nanosheets enhanced the Mitomycin C loading capacity by 274.35%. The increased drug release of 45.1% and 69.8% was also observed at pH 7.4 and 5.0, respectively, after modification. The thioglycolic acid-modified bismuth nanosheets could also be employed for CT scan imaging and synergetic chemo-photo-radiotherapy of cancer cells, displaying its efficiency in biomedical applications. The applications of monoelemental bismuthene benefit from its advantages of various unique properties, such as electrical properties, optical properties and biocompatible property. The tunable bandgap from about 0 eV to 0.55 eV with high carrier mobility and intrinsic stability of bismuthene makes it a suitable material for applications such as electrocatalysis, batteries and supercapacitors. The carrier mobility values of up to 1000 $cm^2\ V^{-1}\ s^{-1}$ played a crucial role in these applications and the two-dimensional structure provides an ideal characteristic for charge transfer, making bismuthene an efficient catalyst. Theoretical studies have shown that bismuthene can exhibit a small adsorption

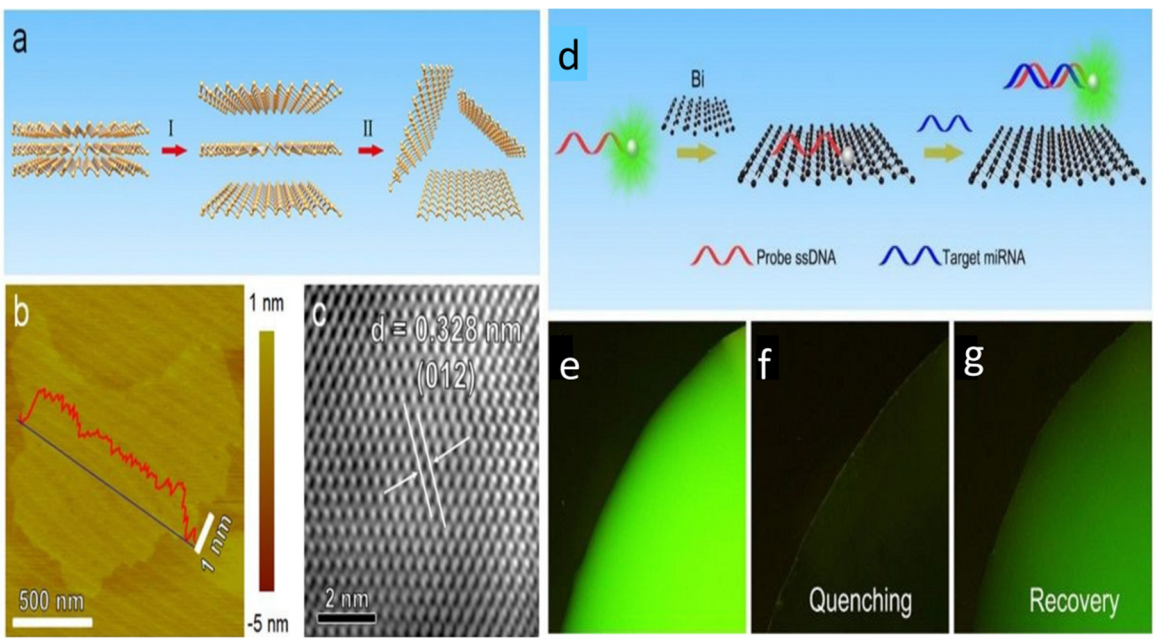

Fig. 13 (a) Schematic depiction of the preparation process of bismuthene nanosheets. (I) Bismuth solution was treated by probe sonication. (II) The solution was centrifuged, and the supernatant containing bismuthene was collected. (b) AFM topography showing few-layer bismuthene. (c) HRTEM image of few-layer bismuthene nanosheets. (d) Schematic illustration of bismuthene nanosheet-based miRNA detection. (e) Fluorescence image of FAM-ssDNA probe solution (10^{-6} M) before mixing with bismuthene. (f) Fluorescence image of FAM-ssDNA probe solution after mixing with bismuthene. (g) Fluorescence image of FAM-ssDNA after mixing with bismuthene and incubation with miRNA-21. Reprinted with permission from RSC.[15]

Table 1 Brief summary of different the applications of bismuthene

Application	Material	Results	Ref.
Supercapacitors	Bismuthene and activated carbon	The maximum specific capacity of 87.3 mA h g^{-1} at 1 A g^{-1} with an energy density of 27.23 W h kg^{-1} and power density of 312.5 W kg^{-1} was achieved.	103
	Bismuthene-graphene	The specific capacitance of 400.83 F g^{-1} at 0.67 A g^{-1} with the energy density of 45.55 W h kg^{-1} at 400 W kg^{-1}, along with a cycling stability of 89.24% after 3600 cycles was reported.	105
	Bismuthene–carbon nanotubes composite	The volumetric capacity of 68.7 F cm^3 was observed with a volumetric power of 203.2 W cm^3 and energy density of 9.5 mW h cm^3	106
Batteries	Buckled bismuthene	Theoretical capacities of 2276 mA h g^{-1}, 2149 mA h g^{-1}, and 1896 mA h g^{-1} were found when used as an anode material for Li, Na and K ion batteries, respectively.	108
	β-Bismuthene/graphene heterostructure	A higher stiffness (369.2 N m^{-1}) and conductivity with the diffusion barrier of 0.32 eV and volume expansion ratio of 4% were observed as an anode material in Li-ion battery.	109
	Bismuthene in PEO electrolyte	The enhanced ionic conductivity and reduced diffusion barrier of Li^+ with stable cycling for 1000 h with current density of 0.2 mA cm^{-2} were achieved.	110
Electrochemical hydrogen evolution	Bismuth nanosheets	The overpotential value of −958 mV at a current density of 10 mA cm^{-2} and the Tafel slope of 122 mV dec^{-1} was achieved for electrocatalytic hydrogen evolution.	82
Electrochemical sensing	Bismuthene and few-layer graphene	The limit of detection of 0.3 mg L^{-1} for both lead and cadmium was attained.	42
	Bismuthene and carbon	Achieved the limit of detection of 0.06 μg L^{-1} and 0.07 μg L^{-1} for lead and cadmium ions, respectively.	83
Electrochemical CO_2 reduction	Bismuthene	Nearly 100% faradaic efficiency and current densities larger than 300 mA cm^{-2} were observed for formate production.	89
	Free-standing 2D bismuth nanosheets	For CO_2 reduction, faradaic efficiency of 99% at −580 mV, durability of >75 hours and small onset overpotential of <90 mV were attained.	18
	Bismuthene	Cathodic energy efficiency of >60% and Faraday efficiency of >90% at wide range of current densities from 50 to 400 mA cm^{-2} were found.	63
	Bismuthene nanosheet arrays grown on copper	The selectivity of >90% and partial current density of 45 mA cm^{-2} were reported.	90
	Interconnected bismuth nanosheet arrays	faradaic efficiency of 90% and current density >300 mA cm^{-2} were achieved with long-term stability, prominent selectivity and high formate partial current density.	91
	Bismuthene	The current density of up to 560 mA cm^{-2} with remarkable continuous operation for more than 500 hours was attained for formate production.	92
Photocatalytic CO_2 reduction	Bismuthene and $CsPbBr_3$ quantum dot S-scheme heterojunction	The yield of 157.76 μmol g^{-1} and 215.56 μmol g^{-1} for CO and CH_4 was observed under UV-visible light irradiation, respectively.	93
Optoelectronic applications	Bismuth 2D sheets on Si substrate	The electrical conductivity, thermal conductivity and Seebeck coefficient were measured to be 46250 S m^{-1}, 1.25 W m^{-1} K^{-1} and −237 μV K^{-1} at room temperature, respectively.	95
	Few-layer bismuthene nanosheets	The pulse width of 361 ns and maximum absorbed pump power of 3.55 W were achieved with the peak power 1.52 W and the repetition rate of 365 kHz when used as a saturable absorber.	4
	Bismuthene quantum dots	The minimum pulse width of 440 ns and the repetition rate of 94 kHz with a peak power of 8.1 W and maximum single pulse energy of 4.5 μJ were attained.	78
	Bismuthene quantum dots	As a saturable absorber, the repetition rate of 457 kHz and pulse duration of 155 ns at 1.34 μm were observed.	48
	Bismuthene	The modulation depth and the saturation intensity of 1% and 2.4 MW cm^{-2} were achieved by depositing bismuthene nanosheets on microfibers.	96
	Few-layer bismuthene	The attained saturable intensity was 110 MW cm^{-2} with a modulation depth of 2.5%.	97
Photovoltaic application	Bismuthene-graphitic carbon nitride composite	The energy density of 31.597 μW h cm^{-2} with the power density of 3.25 MW cm^{-2} and energy storage efficiency of 68.35% was observed.	98

Table 1 (*continued*)

Application	Material	Results	Ref.
	Bismuthene–SnO_2 heterojunction	The heterojunction was applied as an electron transport material in perovskite solar cells to achieve the power conversion efficiency of 18.75%.	99
Biomedical applications	Bi@gelatine nanoparticles	Enhanced CT signal with and excellent CT imaging.	115
	Ultrasmall BiOI nanoparticles	It was observed that the X-ray attenuation was higher than iohexol when used as a contrast agent.	124
	Bismuthene/bismuth oxide-based nano-heterostructure	Successful oxygen-independent tumor ablation with 660 nm irradiation was attained with improved tumor tissue penetration and increased cellular uptake.	125
	Bismuthene nanosheets	Improved cellular uptake photocatalytic and conversion of CO_2 to CO in cancer cells were both studied for cancer treatment.	11
	PVP-encapsulated bismuthene quantum dots	Power of 1.3 W cm^{-2} and the photothermal conversion efficiency of about 30% were attained for 808 nm laser irradiation.	126
	Phase-change material-coated Bi nanodots on the surface of dendritic mesoporous silica nanoparticles	Successful heat-induced photothermal therapy was achieved.	127
	Ultrathin bismuthene nanosheet	The quantitative and specific detection of microRNA with a detection limit of up to 60 pM was attained.	15

energy of 1–3.9 eV for gases, making it a promising catalyst for the oxygen reduction reaction (ORR), hydrogen evolution reaction (HER), and CO_2 reduction reaction (CO_2RR).

The presence of a bandgap also influences the absorption of bismuthene, which plays a major role in photocatalysis and optoelectronic applications. As shown by Zhang *et al.*,[93] photocatalytic CO_2 reduction can be performed under UV-visible irradiation because of its electronic band structure. The ultrafast response time in the order of picoseconds (ps) or subpicoseconds (sub-ps) paves the path towards highly efficient bismuthene-based optical modulators and ultrafast photodetectors in the future. The high optical nonlinearity of bismuthene arises from its strongly anisotropic electronic structure, making it a promising material for use as a saturable absorber in ultrafast laser applications. The biomedical applications of bismuthene such as drug delivery, cancer treatment, contrast agents and bioimaging are possible because of its biocompatibility, antibacterial property and strong X-ray attenuation properties. The photothermal conversion efficiency of 30% has been achieved for photothermal therapy using bismuthene quantum dots. Also, the thin structure of bismuth nanosheets can enable their easy navigation in the body and their high surface area makes them an ideal substrate for surface functionalization to attach drug molecules (Table 1). The different applications of bismuthene and its composites are listed in Table 1.

5. Conclusion and future perspectives

Bismuthene is an attractive monoelemental material in energy-based applications, which has been used as an anode material for rechargeable ion batteries due to its excellent theoretical volumetric capacity and low toxicity.[35] Theoretical studies suggest the strong capacities of bismuthene, bismuthene/graphene heterostructures, and bismuthene/PEO for Li/Na/K batteries. In bismuthene, its interlayer distance is 3.979 Å, which can accommodate the diffusion of Li (1.52 Å) and Na (2.04 Å).[5] Bismuthene and bismuthene-activated carbon showed a gravimetric capacity of 350 mA h g^{-1} and specific capacity of 87.3 mA h g^{-1}, respectively, and bismuthene/graphene presented a specific capacitance of 400.83 F g^{-1} due to the dual improved ion transfer due to the dual transport channel design. The unique favorable physical properties of bismuthene show potential for new device applications with a combination of high speed and energy efficiency. The huge surface of bismuthene acts as catalytic sites and insertion channels. This property makes bismuthene attractive for application in rechargeable batteries. Owing to the large surface area and puckered honeycomb 2D structure of bismuthene, it has potential for drug delivery, and due to its large Bi content, contributes better computerized tomography (CT) imaging capabilities.[128] Owing to its improved biocompatibility and low toxicity, bismuthene has many possible uses in biomedicine. Bismuthene nanoparticles, PVP-coated bismuthene nanodots, Bi@Gel, HA-BiOI, Bi/BiOx, and PVP-BiQDs have been reported to show improved CT imaging resolution and PDT enhancement and also used in CDT therapy and photothermal agents for PTT. Considering its tunable band gap, electronic properties and many other qualities, bismuthene is an attractive candidate for catalysis.[129] Bismuthene, as a narrow band gap nanomaterial, has favorable photothermal conversion efficiency in the mid infrared region and infrared region, and thus it can be employed in various catalytic processes.[130] Due to their absorption features, bismuthene quantum dots were successfully prepared and applied in a 2 μm solid-state pulse laser as an optical modulator.[78] Bismuthene exhibited a lower potential value of −958 mV for the electrochemical hydrogen evolution reaction compared to the bulk material and also bismuthene with graphene, bismuthene-carbon, and bismuthene with different thicknesses showed good electrochemical sensing activity for Cd^{2+} and Pb^{2+} with an LOD of

0.3 mg L^{-1}, which is ascribed to its high surface area and high carrier mobility. Bismuthene, bismuthene on copper and bismuthene-$CsPbBr_3$ QD heterojunction showed activity for CO_2 reduction to formate with good stability and current density. Few-layer bismuthene showed UV and IR absorption and PL responses due to confinement effects and crystal dislocation, and additionally showed electrical and thermal conductivity, which can be used in electronic devises. Theoretical studies illustrate that bismuthene exhibits adsorption activity towards toxic gases such as CO, CO_2, SO, SO_2, NH_3, H_2S, NO_2 and PH_3 due to its strong adsorption energies. However, the experimental research on bismuthene to understand its properties is less compared to the theoretical studies, which has to be explored further. Additionally, different preparation techniques and the application of bismuthene and its composites, heterostructures, doped materials, and core–shells still need to be investigated in various fields such as catalysis, energy production, energy storage, sensing and biomedicine given that the related reports are limited. The large-scale production of bismuthene through a simple and economical synthesis route connects bismuthene to industrial-level use. Bismuthene can be extended to large-scale production and real-time applications owing to its low toxicity, stability and environmental compatibility. Furthermore, the improvement in catalytic activity in the known catalytic systems to extend their large-scale applications is challenging.

Conflicts of interest

Authors declares no conflicts of interest.

Acknowledgements

Authors acknowledges TARE project (TAR/2019/000042) for funding support and Jain (Deemed-to-be-University) JU/MRP/CNMS/12/2022 for the financial and infrastructure support.

References

1 S. Noreen, M. B. Tahir, A. Hussain, T. Nawaz, J. U. Rehman, A. Dahshan, M. Alzaid and H. Alrobei, Emerging 2D-Nanostructured materials for electrochemical and sensing Application-A review, *Int. J. Hydrogen Energy*, 2022, **47**, 1371–1389.

2 Y. Wang, W. Feng, M. Chang, J. Yang, Y. Guo, L. Ding, L. Yu, H. Huang, Y. Chen and J. Shi, Engineering 2D Multifunctional Ultrathin Bismuthene for Multiple Photonic Nanomedicine, *Adv. Funct. Mater.*, 2021, **31**, 2005093.

3 P. Guo, X. Li, T. Chai, T. Feng, Y. Ge, Y. Song and Y. Wang, Few-layer bismuthene for robust ultrafast photonics in C-Band optical communications, *Nanotechnology*, 2019, **30**, 354002.

4 H. Chen, M. Zhou, P. Zhang, H. Yin, S. Zhu, Z. Li and Z. Chen, Passively Q-switched Nd:GYAP laser at 1.3 μm with bismuthene nanosheets as a saturable absorber, *Infrared Phys. Technol.*, 2022, **121**, 104023.

5 T. Wang, H. Wang, Z. Kou, W. Liang, X. Luo, F. Verpoort, Y.-J. Zeng and H. Zhang, Xenes as an Emerging 2D Monoelemental Family: Fundamental Electrochemistry and Energy Applications, *Adv. Funct. Mater.*, 2020, **30**, 2002885.

6 J. Wu, J. Fan, X. Zhao, Y. Wang, D. Wang, H. Liu, L. Gu, Q. Zhang, L. Zheng, D. J. Singh, X. Cui and W. Zheng, Atomically Dispersed MoO_x on Rhodium Metallene Boosts Electrocatalyzed Alkaline Hydrogen Evolution, *Angew. Chem., Int. Ed.*, 2022, **61**, e202207512.

7 G. Wu, X. Han, J. Cai, P. Yin, P. Cui, X. Zheng, H. Li, C. Chen, G. Wang and X. Hong, In-plane strain engineering in ultrathin noble metal nanosheets boosts the intrinsic electrocatalytic hydrogen evolution activity, *Nat. Commun.*, 2022, **13**, 4200.

8 J. Fan, Z. Feng, Y. Mu, X. Ge, D. Wang, L. Zhang, X. Zhao, W. Zhang, D. J. Singh, J. Ma, L. Zheng, W. Zheng and X. Cui, Spatially Confined PdHx Metallenes by Tensile Strained Atomic Ru Layers for Efficient Hydrogen Evolution, *J. Am. Chem. Soc.*, 2023, **145**, 5710–5717.

9 A. K. Nayak, J. Reiner, R. Queiroz, H. Fu, C. Shekhar, B. Yan, C. Felser, N. Avraham and H. Beidenkopf, Resolving the topological classification of bismuth with topological defects, *Sci. Adv.*, 2019, **5**, eaax6996.

10 J. Gou, L. Kong, X. He, Y. L. Huang, J. Sun, S. Meng, K. Wu, L. Chen and A. T. S. Wee, The effect of moiré superstructures on topological edge states in twisted bismuthene homojunctions, *Sci. Adv.*, 2020, **6**, eaba2773.

11 Y. Zhu, Y. Wu, S. Li, X. Yuan, J. Shen, S. Luo, Z. Wang, R. Gao, J. Wu and L. Ge, Photocatalytic and photothermal bismuthene nanosheets as drug carrier capable of generating CO to improve drug sensitivity and reduce inflammation for enhanced cancer therapy, *Chem. Eng. J.*, 2022, **446**, 137321.

12 Z. Xie, B. Zhang, Y. Ge, Y. Zhu, G. Nie, Y. Song, C. K. Lim, H. Zhang and P. N. Prasad, Chemistry, Functionalization, and Applications of Recent Monoelemental Two-Dimensional Materials and Their Heterostructures, *Chem. Rev.*, 2022, **122**, 1127–1207.

13 R. Bhuvaneswari, V. Nagarajan and R. Chandiramouli, Electronic properties of novel bismuthene nanosheets with adsorption studies of G-series nerve agent molecules – a DFT outlook, *Phys. Lett. A*, 2019, **383**, 125975.

14 M. Guo, X. Zhang, J. Liu, F. Gao, X. Zhang, X. Hu, B. Li, X. Zhang, H. Zhou, R. Bai, Y. Wang, J. Li, Y. Liu, Z. Gu and C. Chen, Few-Layer Bismuthene for Checkpoint Knockdown Enhanced Cancer Immunotherapy with Rapid Clearance and Sequentially Triggered One-for-All Strategy, *ACS Nano*, 2020, **14**, 15700–15713.

15 T. Xue, S. R. Bongu, H. Huang, W. Liang, Y. Wang, F. Zhang, Z. Liu, Y. Zhang, H. Zhang and X. Cui, Ultrasensitive detection of microRNA using a bismuthene-enabled fluorescence quenching biosensor, *Chem. Commun.*, 2020, **56**, 7041–7044.

16 X. Yu, W. Liang, C. Xing, K. Chen, J. Chen, W. Huang, N. Xie, M. Qiu, X. Yan, Z. Xie and H. Zhang, Emerging 2D

pnictogens for catalytic applications: status and challenges, *J. Mater. Chem. A*, 2020, **8**, 12887–12927.
17 W. Tao, N. Kong, X. Ji, Y. Zhang, A. Sharma, J. Ouyang, B. Qi, J. Wang, N. Xie, C. Kang, H. Zhang, O. C. Farokhzad and J. S. Kim, Emerging two-dimensional monoelemental materials (Xenes) for biomedical applications, *Chem. Soc. Rev.*, 2019, **48**, 2891–2912.
18 F. Yang, A. O. Elnabawy, R. Schimmenti, P. Song, J. Wang, Z. Peng, S. Yao, R. Deng, S. Song, Y. Lin, M. Mavrikakis and W. Xu, Bismuthene for highly efficient carbon dioxide electroreduction reaction, *Nat. Commun.*, 2020, **11**, 1088.
19 E. Aktürk, O. Ü. Aktürk and S. Ciraci, Single and bilayer bismuthene: stability at high temperature and mechanical and electronic properties, *Phys. Rev. B*, 2016, **94**, 014115.
20 R. Chai, L. Yu, C. Dong, Y. Yin, S. Wang, Y. Chen and Q. Zhang, Oxygen-evolving photosynthetic cyanobacteria for 2D bismuthene radiosensitizer-enhanced cancer radiotherapy, *Bioactive Mater.*, 2022, **17**, 276–288.
21 O. H. Basyouni, M. Abdelfatah, M. E. El-Khouly, T. Mohamed, A. El-Shaer and W. Ismail, Facile and environmentally friendly fabrication of few-layer bismuthene by electrochemical exfoliation method for ultrafast photonic applications, *J. Alloys Compd.*, 2021, **882**, 160766.
22 K. Yaegashi, K. Sugawara, T. Kato, T. Takahashi and T. Sato, Selective Fabrication of Bismuthene and α-Bi on Hydrogen-Terminated SiC(0001), *Langmuir*, 2022, **38**, 13401–13406.
23 X. Liu, S. Zhang, S. Guo, B. Cai, S. A. Yang, F. Shan, M. Pumera and H. Zeng, Advances of 2D bismuth in energy sciences, *Chem. Soc. Rev.*, 2020, **49**, 263–285.
24 C. Wang, L. Wang, X. Li, W. Luo, T. Feng, Y. Zhang, P. Guo and Y. Ge, Few-layer bismuthene for femtosecond soliton molecules generation in Er-doped fiber laser, *Nanotechnology*, 2019, **30**, 025204.
25 D. Kecik, V. O. Özçelik, E. Durgun and S. Ciraci, Structure dependent optoelectronic properties of monolayer antimonene, bismuthene and their binary compound, *Phys. Chem. Chem. Phys.*, 2019, **21**, 7907–7917.
26 Y. Hong, J. Deng, X. Ding, J. Sun and J. Z. Liu, Size Limiting Elemental Ferroelectricity in Bi Nanoribbons: Observation, Mechanism, and Opportunity, *J. Phys. Chem. Lett.*, 2023, **14**, 3160–3167.
27 D. K. Nguyen, T. V. Bao, N. A. Kha, R. Ponce-Pérez, J. Guerrero-Sanchez and D. M. Hoat, Searching for d0 spintronic materials: bismuthene monolayer doped with IVA-group atoms, *RSC Adv.*, 2023, **13**, 5885–5892.
28 E. V. C. Lopes, E. Vernek and T. M. Schmidt, RKKY interactions mediated by topological states in transition metal doped bismuthene, *J. Appl. Phys.*, 2023, **133**, 115105.
29 A. A. Kistanov, S. K. Khadiullin, K. Zhou, S. V. Dmitriev and E. A. Korznikova, Environmental stability of bismuthene: oxidation mechanism and structural stability of 2D pnictogens, *J. Mater. Chem. C*, 2019, **7**, 9195–9202.
30 M. Z. Mohamad Nasir and M. Pumera, Emerging monoelemental 2D nanomaterials for electrochemical sensing applications: from borophene to bismuthene, *TrAC, Trends Anal. Chem.*, 2019, **121**, 115696.
31 M.-Y. Liu, Y. Huang, Q.-Y. Chen, Z.-Y. Li, C. Cao and Y. He, Strain and electric field tunable electronic structure of buckled bismuthene, *RSC Adv.*, 2017, **7**, 39546–39555.
32 I. Torres, A. M. Villa-Manso, M. Revenga-Parra, C. Gutiérrez-Sánchez, D. A. Aldave, E. Salagre, E. G. Michel, M. Varela, J. Gómez-Herrero, E. Lorenzo, F. Pariente and F. Zamora, Preparation of high-quality few-layers bismuthene hexagons, *Appl. Mater. Today*, 2022, **26**, 101360.
33 S. Noreen, M. B. Tahir, A. Hussain, T. Nawaz, J. U. Rehman, A. Dahshan, M. Alzaid and H. Alrobei, Emerging 2D-Nanostructured materials for electrochemical and sensing Application-A review, *Int. J. Hydrogen Energy*, 2021, **47**(2), 1371–1389.
34 P. Gao, Y. Xiao, L. Li, W. Li and W. Tao, Biomedical applications of 2D monoelemental materials formed by group VA and VIA: a concise review, *J. Nanobiotechnol.*, 2021, **19**, 1–23.
35 Z. Huang, H. Liu, R. Hu, H. Qiao, H. Wang, Y. Liu, X. Qi and H. Zhang, Structures, properties and application of 2D monoelemental materials (Xenes) as graphene analogues under defect engineering, *Nano Today*, 2020, **35**, 100906.
36 Z. Wu and J. Hao, Electrical transport properties in group-V elemental ultrathin 2D layers, *npj 2D Mater. Appl.*, 2020, **4**, 1–13.
37 K. Khan, A. K. Tareen, M. Iqbal, L. Wang, C. Ma, Z. Shi, Z. Ye, W. Ahmad, R. U. R. Sagar and S. S. Shams, Navigating recent advances in monoelemental materials (Xenes)-fundamental to biomedical applications, *Prog. Solid State Chem.*, 2021, **63**, 100326.
38 P. K. Roy, J. Luxa and Z. Sofer, Emerging pnictogen-based 2D semiconductors: sensing and electronic devices, *Nanoscale*, 2020, **12**, 10430–10446.
39 T. Wang, H. Wang, Z. Kou, W. Liang, X. Luo, F. Verpoort, Y. J. Zeng and H. Zhang, Xenes as an emerging 2D monoelemental family: fundamental electrochemistry and energy applications, *Adv. Funct. Mater.*, 2020, **30**, 2002885.
40 L. Lu, Z. Liang, L. Wu, Y. Chen, Y. Song, S. C. Dhanabalan, J. S. Ponraj, B. Dong, Y. Xiang and F. Xing, Few-layer bismuthene: sonochemical exfoliation, nonlinear optics and applications for ultrafast photonics with enhanced stability, *Laser Photonics Rev.*, 2018, **12**, 1700221.
41 H. Chen, M. Zhou, P. Zhang, H. Yin, S. Zhu, Z. Li and Z. Chen, Passively Q-switched Nd: GYAP laser at 1.3 μm with bismuthene nanosheets as a saturable absorber, *Infrared Phys. Technol.*, 2022, **121**, 104023.
42 A. C. Lazanas, K. Tsirka, A. S. Paipetis and M. I. Prodromidis, 2D bismuthene/graphene modified electrodes for the ultra-sensitive stripping voltammetric determination of lead and cadmium, *Electrochim. Acta*, 2020, **336**, 135726.
43 R. Gusmão, Z. Sofer, D. Bouša and M. Pumera, Pnictogen (As, Sb, Bi) nanosheets for electrochemical applications are produced by shear exfoliation using kitchen blenders, *Angew. Chem.*, 2017, **129**, 14609–14614.
44 H. L. Chia, N. M. Latiff, R. Gusmão, Z. Sofer and M. Pumera, Cytotoxicity of shear exfoliated pnictogen (As, Sb, Bi) nanosheets, *Chem. – Eur. J.*, 2019, **25**, 2242–2249.

45 C. C. Mayorga-Martinez, R. Gusmão, Z. Sofer and M. Pumera, Pnictogen-based enzymatic phenol biosensors: phosphorene, arsenene, antimonene, and bismuthene, *Angew. Chem., Int. Ed.*, 2019, **58**, 134–138.
46 Y. Wang, W. Huang, J. Zhao, H. Huang, C. Wang, F. Zhang, J. Liu, J. Li, M. Zhang and H. Zhang, A bismuthene-based multifunctional all-optical phase and intensity modulator enabled by photothermal effect, *J. Mater. Chem. C*, 2019, **7**, 871–878.
47 H. Pan, W. Huang, H. Chu, Y. Li, S. Zhao, G. Li, H. Zhang and D. Li, Bismuthene quantum dots based optical modulator for MIR lasers at 2 μm, *Opt. Mater.*, 2020, **102**, 109830.
48 L. Dong, W. Huang, H. Chu, Y. Li, Y. Wang, S. Zhao, G. Li, H. Zhang and D. Li, Passively Q-switched near-infrared lasers with bismuthene quantum dots as the saturable absorber, *Opt. Laser Technol.*, 2020, **128**, 106219.
49 N. Hussain, T. Liang, Q. Zhang, T. Anwar, Y. Huang, J. Lang, K. Huang and H. Wu, Ultrathin Bi nanosheets with superior photoluminescence, *Small*, 2017, **13**, 1701349.
50 K. Khan, A. K. Tareen, Q. U. Khan, M. Iqbal, H. Zhang and Z. Guo, Novel synthesis, properties and applications of emerging group VA two-dimensional monoelemental materials (2D-Xenes), *Mater. Chem. Front.*, 2021, **5**, 6333–6391.
51 M. Jankowski, D. Kamiński, K. Vergeer, M. Mirolo, F. Carla, G. Rijnders and T. R. Bollmann, Controlling the growth of Bi(110) and Bi(111) films on an insulating substrate, *Nanotechnology*, 2017, **28**, 155602.
52 S. Yaginuma and T. Nagao, Softening versus hardening transition in surface bilayer bonding of bismuth nanofilm, *Phys. Rev. B: Condens. Matter Mater. Phys.*, 2010, **82**, 045422.
53 F. Song, J. W. Wells, Z. Jiang, M. Saxegaard and E. Wahlström, Low-temperature growth of bismuth thin films with (111) facet on highly oriented pyrolytic graphite, *ACS Appl. Mater. Interfaces*, 2015, **7**, 8525–8532.
54 H. Zhao, X. Sun, Z. Zhu, W. Zhong, D. Song, W. Lu and L. Tao, Physical vapor deposited 2D bismuth for CMOS technology, *J. Semiconductors*, 2020, **41**, 081001.
55 D. Lu, S. Luo, S. Liu, H. Yao, X. Ren, W. Zhou, D. Tang, X. Qi and J. Zhong, Anomalous temperature-dependent Raman scattering of vapor-deposited two-dimensional Bi thin films, *J. Phys. Chem. C*, 2018, **122**, 24459–24466.
56 R. K. Jain, J. Kaur, S. Arora, A. Kumar, A. K. Chawla and A. Khanna, Effects of oblique angle deposition on structural, electrical and wettability properties of Bi thin films grown by thermal evaporation, *Appl. Surf. Sci.*, 2019, **463**, 45–51.
57 P. Vishnoi, K. Pramoda and C. N. R. Rao, 2D Elemental Nanomaterials Beyond Graphene, *ChemNanoMat*, 2019, **5**, 1062–1091, DOI: **10.1002/cnma.201900176**.
58 X. Qin, C. Sui and L. Di, Influence of substrate temperature on the morphology and structure of bismuth thin films deposited by magnetron sputtering, *Vacuum*, 2019, **166**, 316–322.
59 C. M. Bedoya-Hincapié, J. de la Roche, E. Restrepo-Parra, J. E. Alfonso and J. J. Olaya-Florez, Structural and morphological behavior of bismuth thin films grown through DC-magnetron sputtering, *Ingeniare. Revista chilena de ingeniería*, 2015, **23**, 92–97.
60 Z. Yang, Z. Wu, Y. Lyu and J. Hao, Centimeter-scale growth of two-dimensional layered high-mobility bismuth films by pulsed laser deposition, *InfoMat*, 2019, **1**, 98–107.
61 S. Rodil, O. Garcia-Zarco, E. Camps, H. Estrada, M. Lejeune, L. Bourja and A. Zeinert, Preferential orientation in bismuth thin films as a function of growth conditions, *Thin Solid Films*, 2017, **636**, 384–391.
62 S. Zhao, Y. Zhang and Z. Zang, Room-temperature doping of ytterbium into efficient near-infrared emission CsPbBr1.5Cl1.5 perovskite quantum dots, *Chem. Commun.*, 2020, **56**, 5811–5814.
63 B. Ning, Q. Xu, M. Liu, H. Jiang, Y. Hu and C. Li, Bismuthene with stable BiO bonds for efficient CO_2 electroreduction to formate, *Chem. Eng. Sci.*, 2022, **251**, 117409.
64 I. Torres, A. M. Villa-Manso, M. Revenga-Parra, C. Gutiérrez-Sánchez, D. A. Aldave, E. Salagre, E. G. Michel, M. Varela, J. Gómez-Herrero and E. Lorenzo, Preparation of high-quality few-layers bismuthene hexagons, *Appl. Mater. Today*, 2022, **26**, 101360.
65 S. Mourdikoudis, N. Antonatos, V. Mazánek, I. Marek and Z. K. Sofer, Simple Bottom-Up Synthesis of Bismuthene Nanostructures with a Suitable Morphology for Competitive Performance in the Electrocatalytic Nitrogen Reduction Reaction, *Inorg. Chem.*, 2022, **61**, 5524–5538.
66 M. S. Ozer, Z. Eroglu, A. S. Yalin, M. Kılıç, U. Rothlisberger and O. Metin, Bismuthene as a versatile photocatalyst operating under variable conditions for the photoredox CH bond functionalization, *Appl. Catal., B*, 2022, **304**, 120957.
67 O. H. Basyouni, M. Abdelfatah, M. E. El-Khouly, T. Mohamed, A. El-Shaer and W. Ismail, Advances of 2D bismuth in energy sciences, *J. Alloys Compd.*, 2021, **882**, 160766.
68 J. Fan, X. Zhao, X. Mao, J. Xu, N. Han, H. Yang, B. Pan, Y. Li, L. Wang and Y. Li, Large-Area Vertically Aligned Bismuthene Nanosheet Arrays from Galvanic Replacement Reaction for Efficient Electrochemical CO_2 Conversion, *Adv. Mater.*, 2021, **33**, 2100910.
69 L. Li, C. Tang, B. Xia, H. Jin, Y. Zheng and S.-Z. Qiao, Two-dimensional mosaic bismuth nanosheets for highly selective ambient electrocatalytic nitrogen reduction, *ACS Catal.*, 2019, **9**, 2902–2908.
70 X. Liu, S. Zhang, S. Guo, B. Cai, S. A. Yang, F. Shan, M. Pumera and H. Zeng, Advances of 2D bismuth in energy sciences, *Chem. Soc. Rev.*, 2020, **49**, 263–285.
71 Á. Y. Aguilera, G. Krepper and M. S. Di Nezio, Simple One-Step Synthesis of Bismuth Nanoparticles for Voltammetric Sensing of Metal Ions, *J. Cluster Sci.*, 2022, **33**, 1417–1426.
72 B. Wei, X. Zhang, C. Zhang, Y. Jiang, Y.-Y. Fu, C. Yu, S.-K. Sun and X.-P. Yan, Facile Synthesis of Uniform-Sized Bismuth Nanoparticles for CT Visualization of Gastrointestinal Tract in Vivo, *ACS Appl. Mater. Interfaces*, 2016, **8**, 12720–12726.
73 R. Vazquez-Munoz, M. J. Arellano-Jimenez and J. L. Lopez-Ribot, Bismuth nanoparticles obtained by a facile synthesis

method exhibit antimicrobial activity against Staphylococcus aureus and Candida albicans, *BMC Biomed. Eng.*, 2020, **2**, 11.

74 J. Wu, F. Qin, Z. Lu, H.-J. Yang and R. Chen, Solvothermal synthesis of uniform bismuth nanospheres using poly(N-vinyl-2-pyrrolidone) as a reducing agent, *Nanoscale Res. Lett.*, 2011, **6**, 66.

75 K. Petsom, A. Kopwitthaya, M. Horphathum, J. Kaewkhao, N. Sangwaranatee and H. Kim, Facile method for bismuth nanorod synthesis, *Mater. Today: Proc.*, 2018, **5**, 14960–14964.

76 H. Long, X. Yin, X. Wang, Y. Zhao and L. Yan, Bismuth nanorods confined in hollow carbon structures for high performance sodium- and potassium-ion batteries, *J. Energy Chem.*, 2022, **67**, 787–796.

77 F. Wang, R. Tang, H. Yu, P. C. Gibbons and W. E. Buhro, Size- and Shape-Controlled Synthesis of Bismuth Nanoparticles, *Chem. Mater.*, 2008, **20**, 3656–3662.

78 H. Pan, W. Huang, H. Chu, Y. Li, S. Zhao, G. Li, H. Zhang and D. Li, Bismuthene quantum dots based optical modulator for MIR lasers at 2 μm, *Opt. Mater.*, 2020, **102**, 109830.

79 R. Fu, S. Xu, Y.-N. Lu and J.-J. Zhu, Synthesis and Characterization of Triangular Bismuth Nanoplates, *Cryst. Growth Des.*, 2005, **5**, 1379–1385.

80 C. Lu, R. Li, Z. Miao, F. Wang and Z. Zha, Emerging metallenes: synthesis strategies, biological effects and biomedical applications, *Chem. Soc. Rev.*, 2023, **52**, 2833–2865.

81 S. Gong, H. Liu, F. Zhao, Y. Zhang, H. Xu, M. Li, J. Qi, H. Wang, C. Li, W. Peng, X. Fan and J. Liu, Vertically Aligned Bismuthene Nanosheets on MXene for High-Performance Capacitive Deionization, *ACS Nano*, 2023, **17**, 4843–4853.

82 C. Duan, H. Liu, Z. Huang, H. Qiao, Y. Zhou, G. Liao, Y. Liu and X. Qi, Two-dimensional Bi nanosheets as an enhanced electrocatalyst for hydrogen evolution reaction, *J. Sol-Gel Sci. Technol.*, 2021, **99**, 132–139.

83 M. A. Tapia, C. Pérez-Ràfols, R. Gusmão, N. Serrano, Z. Sofer and J. M. Díaz-Cruz, Enhanced voltammetric determination of metal ions by using a bismuthene-modified screen-printed electrode, *Electrochim. Acta*, 2020, **362**, 137144.

84 M. Isa, I. Ashfaq, A. Majid, M. Shakil and T. Iqbal, A DFT study of silver decorated bismuthene for gas sensing properties and effect of humidity, *Mater. Sci. Semicond. Process.*, 2022, **145**, 106635.

85 P. Panigrahi, P. K. Panda, Y. Pal, H. Bae, H. Lee, R. Ahuja and T. Hussain, Two-Dimensional Bismuthene Nanosheets for Selective Detection of Toxic Gases, *ACS Appl. Nano Mater.*, 2022, **5**, 2984–2993.

86 Y. Zhang, Y. Qin, L. Jiao, H. Wang, Z. Wu, X. Wei, Y. Wu, N. Wu, L. Hu, H. Zhong, W. Gu and C. Zhu, Atomically thin bismuthene nanosheets for sensitive electrochemical determination of heavy metal ions, *Anal. Chim. Acta*, 2022, **1235**, 340510.

87 A. Chen, Y. Han, Z. Wang, J. Cai, S. Ye and J. Li, Single atom modified two-dimensional bismuthenes for toxic gas detection, *Phys. Chem. Chem. Phys.*, 2023, **25**, 9249–9255.

88 P. Snehha, V. Nagarajan and R. Chandiramouli, Novel bismuthene nanotubes to detect NH_3, NO_2 and PH_3 gas molecules – A first-principles insight, *Chem. Phys. Lett.*, 2018, **712**, 102–111.

89 C. Cao, D.-D. Ma, J.-F. Gu, X. Xie, G. Zeng, X. Li, S.-G. Han, Q.-L. Zhu, X.-T. Wu and Q. Xu, Metal–Organic Layers Leading to Atomically Thin Bismuthene for Efficient Carbon Dioxide Electroreduction to Liquid Fuel, *Angew. Chem., Int. Ed.*, 2020, **59**, 15014–15020.

90 J. Fan, X. Zhao, X. Mao, J. Xu, N. Han, H. Yang, B. Pan, Y. Li, L. Wang and Y. Li, Large-Area Vertically Aligned Bismuthene Nanosheet Arrays from Galvanic Replacement Reaction for Efficient Electrochemical CO_2 Conversion, *Adv. Mater.*, 2021, **33**, 2100910.

91 Y.-C. He, D.-D. Ma, S.-H. Zhou, M. Zhang, J.-J. Tian and Q.-L. Zhu, Integrated 3D Open Network of Interconnected Bismuthene Arrays for Energy-Efficient and Electrosynthesis-Assisted Electrocatalytic CO_2 Reduction, *Small*, 2022, **18**, 2105246.

92 M. Zhang, W. Wei, S. Zhou, D.-D. Ma, A. Cao, X.-T. Wu and Q.-L. Zhu, Engineering a conductive network of atomically thin bismuthene with rich defects enables CO_2 reduction to formate with industry-compatible current densities and stability, *Energy Environ. Sci.*, 2021, **14**, 4998–5008.

93 Y. Zhang, Y. Tian, W. Chen, M. Zhou, S. Ou and Y. Liu, Construction of a Bismuthene/$CsPbBr_3$ Quantum Dot S-Scheme Heterojunction and Enhanced Photocatalytic CO_2 Reduction, *J. Phys. Chem. C*, 2022, **126**, 3087–3097.

94 J. Zhu, H. Chen, Y. Zi, M. Wang and W. Huang, Size-tunable bismuth quantum dots for self-powered photodetectors under ambient conditions, *Nanotechnology*, 2022, **34**, 1–7.

95 W. Zhong, Y. Zhao, B. Zhu, J. Sha, E. S. Walker, S. Bank, Y. Chen, D. Akinwande and L. Tao, Anisotropic thermoelectric effect and field-effect devices in epitaxial bismuthene on Si(111), *Nanotechnology*, 2020, **31**, 475202.

96 T. Feng, X. Li, T. Chai, P. Guo, Y. Zhang, R. Liu, J. Liu, J. Lu and Y. Ge, Bismuthene Nanosheets for 1 μm Multipulse Generation, *Langmuir*, 2020, **36**, 3–8.

97 P. Guo, X. Li, T. Feng, Y. Zhang and W. Xu, Few-Layer Bismuthene for Coexistence of Harmonic and Dual Wavelength in a Mode-Locked Fiber Laser, *ACS Appl. Mater. Interfaces*, 2020, **12**, 31757–31763.

98 G. Maheshwaran, P. Pandi, S. Suganya, B. A. Kumar, G. Ramalingam, M. R. Prabhu and S. Sudhahar, Fabrication of self charging supercapacitor based on two dimensional bismuthene-graphitic carbon nitride nanocomposite powered by dye sensitized solar cells, *J. Energy Storage*, 2022, **56**, 105900.

99 R. Xue, X. Zhou, S. Peng, P. Xu, S. Wang, C. Xu, W. Zeng, Y. Xiong and D. Liang, Architecturing Lattice-Matched Bismuthene–SnO_2 Heterojunction for Effective Perovskite Solar Cells, *ACS Sustainable Chem. Eng.*, 2020, **8**, 10714–10725.

100 Y. Liu, S. Benter, C. S. Ong, R. P. Maciel, L. Bjork, A. Irish, O. Eriksson, A. Mikkelsen and R. Timm, A 2D Bismuth-Induced Honeycomb Surface Structure on GaAs(111), *ACS Nano*, 2023, **17**, 5047–5058.

101 M. Abdelfatah, O. H. Basyouni, W. Ismail and A. El-Shaer, Femtosecond nonlinear optical response and minority carrier lifetime of F4TCNQ-doped bismuthene for optoelectronic and ultrafast photonic applications, *J. Alloys Compd.*, 2023, 936.

102 H. Pan, H. Chu, Y. Li, Z. Pan, J. Zhao, S. Zhao, W. Huang and D. Li, Bismuthene quantum dots integrated D-shaped fiber as saturable absorber for multi-type soliton fiber lasers, *J. Materiomics*, 2023, **9**, 183–190.

103 M. Girirajan, N. B. Alagarsamy, K. Ramachandran, R. P. Manimuthu, D. Pazhanivel, K. K. Muthusamy and S. Sakkarapani, Two dimensional layered bismuthene nanosheets with ultra-fast charge transfer kinetics as a superior electrode material for high performance asymmetric supercapacitor, *Electrochim. Acta*, 2022, **426**, 140838.

104 N. Devi and S. S. Ray, Performance of bismuth-based materials for supercapacitor applications: a review, *Mater. Today Commun.*, 2020, **25**, 101691.

105 N. Wei, Y. Li, Y. Tang, Y. Zhou, R. Ning, M. Tang, S. Lu, W. Zeng and Y. Xiong, Resilient bismuthene-graphene architecture for multifunctional energy storage and wearable ionic-type capacitive pressure sensor device, *J. Colloid Interface Sci.*, 2022, **626**, 23–34.

106 B. Yang, X. Li, Y. Cheng, S. Duan, B. Zhao, W. Yi, C. Wang, H. Sun, Z. Wang, D. Gu, S. Chen and X. Liu, Liquid phase exfoliation of bismuth nanosheets for flexible all-solid-state supercapacitors with high energy density, *J. Mater. Chem. C*, 2020, **8**, 12314–12322.

107 M. Sajjad, S. U. Asif, L. Guan, Y. Jiao, Y. Jiang, L. Zhang, J. Wen, S. Zhang, Y. Lin and S. Zhang, Bismuth Yttrium Oxide (Bi3YO6), A New Electrode Material For Asymmetric Aqueous Supercapacitors, *J. Inorg. Organomet. Polym. Mater.*, 2021, **31**, 1260–1270.

108 M. I. Khan, G. Nadeem, A. Majid and M. Shakil, A DFT study of bismuthene as anode material for alkali-metal (Li/Na/K)-ion batteries, *Mater. Sci. Eng., B*, 2021, **266**, 115061.

109 S. Wang, C. Tang, Y. Huang and J. Gong, Remarkable-cycle-performance β-bismuthene/graphene heterostructure anode for Li-ion battery, *Chin. Chem. Lett.*, 2022, **33**, 3802–3808.

110 L. Xu, J. Li, Y. Xiang, Y. Tian, R. Momen, H. Liu, F. Zhu, H. Tu, Z. Luo, S. Fang, W. Deng, G. Zou, H. Hou and X. Ji, Few-layer bismuthene enabled solid-state Li batteries, *Energy Storage Mater.*, 2022, **52**, 655–663.

111 F. R. Fan, R. Wang, H. Zhang and W. Wu, Emerging beyond-graphene elemental 2D materials for energy and catalysis applications, *Chem. Soc. Rev.*, 2021, **50**, 10983–11031.

112 G. Maheshwaran, M. R. Prabhu, G. Ravi, K. Sankaranarayanan and S. Sudhahar, Probing the energy conversion and storage process in two dimensional layered bismuthene-hexagonal boron nitride nanocomposite electrode and PVA-KOH-$BaTiO_3$ piezoelectrolyte nanogenerators, *Nano Energy*, 2023, **106**, 108060.

113 C. Gomez, G. Hallot, S. Laurent and M. Port, Medical Applications of Metallic Bismuth Nanoparticles, *Pharmaceutics*, 2021, **13**, 1793.

114 J. C. Bulmahn, G. Tikhonowski, A. A. Popov, A. Kuzmin, S. M. Klimentov, A. V. Kabashin and P. N. Prasad, Laser-ablative synthesis of stable aqueous solutions of elemental bismuth nanoparticles for multimodal theranostic applications, *Nanomaterials*, 2020, **10**, 1463.

115 C. Liu, L. Zhang, X. Chen, S. Li, Q. Han, L. Li and C. Wang, Biomolecules-assisted synthesis of degradable bismuth nanoparticles for dual-modal imaging-guided chemo-photothermal therapy, *Chem. Eng. J.*, 2020, **382**, 122720.

116 M. Shakeri, H. Delavari, A. Montazerabadi and A. Yourdkhani, Hyaluronic acid-coated ultrasmall BiOI nanoparticles as a potentially targeted contrast agent for X-ray computed tomography, *Int. J. Biol. Macromol.*, 2022, **217**, 668–676.

117 M. Qiu, D. Wang, H. Huang, T. Yin, W. Bao, B. Zhang, Z. Xie, N. Xie, Z. Wu and C. Ge, A Regioselectively Oxidized 2D Bi/BiOx Lateral Nano-Heterostructure for Hypoxic Photodynamic Therapy, *Adv. Mater.*, 2021, **33**, 2102562.

118 Y. Zhu, Y. Wu, S. Li, X. Yuan, J. Shen, S. Luo, Z. Wang, R. Gao, J. Wu and L. Ge, Photocatalytic and Photothermal Bismuthene Nanosheets as Drug Carrier Capable of Generating CO to Improve Drug Sensitivity and Reduce Inflammation for Enhanced Cancer Therapy, *Chem. Eng. J.*, 2022, 137321.

119 X. Liu, B. Jiang, Y. Liu, L. Liu, T. Xia, X. Zhang, C. Ye, Y. Yu and B. Wang, Two-Dimensional As/BlueP van der Waals Hetero-Structure as a Promising Photocatalyst for Water Splitting: A DFT Study, *Coatings*, 2020, 10.

120 Y. Wang, W. Feng, M. Chang, J. Yang, Y. Guo, L. Ding, L. Yu, H. Huang, Y. Chen and J. Shi, Engineering 2D multifunctional ultrathin bismuthene for multiple photonic nanomedicine, *Adv. Funct. Mater.*, 2021, **31**, 2005093.

121 W. Huang, J. Zhu, M. Wang, L. Hu, Y. Tang, Y. Shu, Z. Xie and H. Zhang, Emerging Mono-Elemental Bismuth Nanostructures: Controlled Synthesis and Their Versatile Applications, *Adv. Funct. Mater.*, 2021, **31**, 2007584.

122 L. Yang, P. Jia, S. Song, Y. Dong, R. Shen, F. He and S. Gai, On-Demand Triggered Chemodynamic Therapy by NIR-II Light on Oxidation-Prevented Bismuth Nanodots, *ACS Appl. Mater. Interfaces*, 2022, 21787–21799.

123 M. Varzandeh, J. Varshosaz, S. Labbaf and N. Esmaeil, Sodium-borohydride exfoliated bismuthene loaded with Mitomycin C for chemo-photo-radiotherapy of triple negative breast cancer, *Int. J. Pharm.*, 2023, **636**, 122825.

124 M. Shakeri, H. Delavari H, A. Montazerabadi and A. Yourdkhani, Hyaluronic acid-coated ultrasmall BiOI nanoparticles as a potentially targeted contrast agent for X-ray computed tomography, *Int. J. Biol. Macromol.*, 2022, **217**, 668–676.

125 M. Qiu, D. Wang, H. Huang, T. Yin, W. Bao, B. Zhang, Z. Xie, N. Xie, Z. Wu, C. Ge, Q. Wang, M. Gu, H. L. Kutscher, L. Liu, S. Bao, P. N. Prasad and H. Zhang, A Regioselectively Oxidized 2D Bi/BiOx Lateral Nano-Heterostructure for Hypoxic Photodynamic Therapy, *Adv. Mater.*, 2021, **33**, 2102562.

126 W. Huang, J. Zhu, M. Wang, L. Hu, Y. Tang, Y. Shu, Z. Xie and H. Zhang, Emerging Mono-Elemental Bismuth Nanostructures: Controlled Synthesis and Their Versatile Applications, *Adv. Funct. Mater.*, 2021, **31**, 2007584.
127 L. Yang, P. Jia, S. Song, Y. Dong, R. Shen, F. He and S. Gai, On-Demand Triggered Chemodynamic Therapy by NIR-II Light on Oxidation-Prevented Bismuth Nanodots, *ACS Appl. Mater. Interfaces*, 2022, **14**, 21787–21799.
128 J. Fan, X. Zhao, X. Mao, J. Xu, N. Han, H. Yang, B. Pan, Y. Li, L. Wang and Y. Li, Large-Area Vertically Aligned Bismuthene Nanosheet Arrays from Galvanic Replacement Reaction for Efficient Electrochemical CO_2 Conversion, *Adv. Mater.*, 2021, **33**, 2100910.
129 S. Guo, Y. Zhang, Y. Ge, S. Zhang, H. Zeng and H. Zhang, 2D V-V Binary Materials: Status and Challenges, *Adv. Mater.*, 2019, **31**, 1902352.
130 Z. Sun, H. Chu, S. Zhao, G. Li and D. Li, Optical properties enhancement of buckled Bismuthene in mid-infrared region: a theoretical first-principle study, *Mol. Simul.*, 2020, **46**, 1004–1010.